**The Dissertation Committee for Linda Letti Lopez Certifies that this is the approved version of the following Dissertation:**

# Early events in the infection cycle of bacteriophage T7

**Committee:**

Ian Molineux, Supervisor

Bryan W. Davies

Ilya J. Finkelstein

Jason McLellan

Chris Sullivan

# Early events in the infection cycle of bacteriophage T7

**by**

**Linda Letti Lopez**

**Dissertation**

Presented to the Faculty of the Graduate School of

The University of Texas at Austin

in Partial Fulfillment

of the Requirements

for the Degree of

**Doctor of Philosophy**

**The University of Texas at Austin**

**July 2023**

## Acknowledgements

I am grateful to my supervisor, Ian Molineux, for allowing me to work in his lab. It is easy to become enthralled with the unknown, but much more difficult to shine light on it so that it is knowable. I am thankful to have born witness to the workings of a well-trained mind and I hope that I can mimic that to some measure in the years to come.

I am grateful to Ilya Finkelstein for his advice and kindness through the years. His frank words, often lyrically phrased, have frequently been a source of light in the darkness.

Most of all, however, I am grateful for the immense bounty of love in my life that has carried me through this strange journey. For my family, adoring and adored, words will never suffice to express my gratitude. For my friends who are my family, my darling Rita, and Manuel, my soul mate, I thank them for loving who I've been, who I am, and for always believing in who I might yet be. Kaylee and Jim, my friendship hub pioneers, have been there to talk science and sorrow, keeping me laughing the whole time—the joy and kindness they've offered has been life-sustaining. I am thankful for those scattered about North America, but in delightful and distractingly constant contact: Agus, Ariel, Britt, Cait, Jojo, Katie, Rachel, Ryan, Stephanie. How lucky I am to have such support, across miles and time zones. And for the folks who were there for informal journal clubs, happy hours, hikes, workout sessions, and venting sessions, I will always be grateful for the reminder that science can be, and should be, a communal endeavor.

# Abstract

## Early events in the infection cycle of bacteriophage T7

Linda Letti Lopez, PhD

The University of Texas at Austin, 2023

Supervisor: Ian Molineux

The emergence of molecular biology as a discipline was dependent on the use of bacteriophages as model organisms. The T-series of phages were first characterized in 1945, and while its members have since been used as tools for probing genetic structure and function, much remains unknown about these phages themselves. This lab has long focused on phage T7, and while we have a superficial understanding about the major processes in its life cycle, in the past decade, advances in imaging technology have allowed not only new insights, but new questions to emerge. In **Chapter 1**, I provide a brief history of phage biology and background on phage T7. In **Chapter 2**, I visit the topic of T7 DNA replication, using an alternative method to investigate timing and quantity. In **Chapter 3**, I describe the observation of an ATP synthase superstructure formed around the phage T7 DNA translocation apparatus, and use a method pioneered in this lab for investigating how ATP synthase might be involved in phage infection. Altogether, this work brings new understanding to the process of phage T7 DNA entry and offers the possibility for the discovery of a new class of biological rotary motors.

# Table of Contents

List of Tables ..... 8

List of Figures ..... 9

**CHAPTER 1: A BRIEF HISTORY OF PHAGE BIOLOGY--WHAT'S PAST IS PROLOGUE ..... 10**

In the beginning was the lytic principle ..... 10

The Phage Group ..... 14

Phage T7 ..... 19

DNA Ejection ..... 20

**CHAPTER 2: T7 DNA REPLICATION REVISITED ..... 26**

Introduction ..... 26

Results ..... 29

Discussion ..... 33

Materials and Methods ..... 34

Bacteria, Phage, and Media: ..... 34

DNA Replication Assay: ..... 34

Analysis of DNA: ..... 35

**CHAPTER 3: PHAGE T7 GENOME ENTRY INVOLVES HOST ATP SYNTHASE ..... 41**

Introduction ..... 42

Results ..... 43

Discussion ..... 50

Materials and Methods ..... 53

Bacteria and Media: ..... 53

Phage: ..... 53

Lysis and one-step growth assays: ..... 54

DNA entry assay: ..... 54

Analysis of DNA: ..... 56

**CHAPTER 4: DISCUSSION ..... 68**

References ..... 71

# List of Tables

Table 3.1. E. coli strains used in this work .....66

Table 3.2. Phages used in this work.....67

# List of Figures

**Figure 2.1**. A model for T7 concatemer formation: .....36

**Figure 2.2**. A direct comparison of methods for assaying *in vivo* DNA replication.....37

**Figure 2.3**. Mature genetic ends change in relative abundance during replication, never recovering to their original proportions: .....39

**Figure 3.1**. Bacteriophage T7 recruits ATP synthase at the initiation of infection.....57

**Fig. 3.2**. Absence of ATP synthase causes a conditional defect for phage T7 .....59

**Figure 3.3**. DNA entry experiments show no obvious role for ATP synthase during bulk T7 genome translocation.....60

**Figure 3.4**. DNA entry experiments show no obvious role for ATP synthase during T7 genome translocation.....62

**Figure 3.5**. Rate of phage T7 DNA entry is slower in a Δatp host when the pH is above or below neutral. In the absence of transcription, disengagement of the T7 gp16 “brake” allows proton flow through ATP synthase to drive rapid phage DNA entry.....64

# CHAPTER 1: A BRIEF HISTORY OF PHAGE BIOLOGY--WHAT'S PAST IS PROLOGUE

The history of molecular biology is intimately tied to the history of phage biology. At the nascence of this field, studies on bacteriophage were widely favored due to the simplicity of phage as a model. Composed of only protein and nucleic acid, with a rapid life cycle, phage offered a simpler and more rapid way to tease out cause and effect compared to using animal or single-celled models. Yet, inevitably, as phage research revealed critical insights into molecular biology, basic knowledge grew, and with it, technical capability. The field moved on as it was empowered to probe more complex systems, and phage research diminished to those passionate few who'd made understanding them their life's work. Yet, with the discovery of CRISPR as a tool for genetic manipulation (Cong et al., 2013; Gasiunas et al., 2012; Jinek et al., 2012), there's been a remarkable revival in phage research. Phage has been recognized not only as a gold mine for the discovery of new molecular tools, but once again have generated interest as primary research subjects. From the discovery of phage "nuclei" (Chaikeeratisak et al., 2017), to non-canonical nucleotides (Pezo et al., 2021; Sleiman et al., 2021; Zhou et al., 2021), to new arsenals of anti-phage defense systems (Bernheim et al., 2021; Bobonis et al., 2022; Cohen et al., 2019; Johnson et al., 2022; Kronheim et al., 2018; Millman et al., 2020; Tal et al., 2021)—phage biology, as it turns out, remains replete with new frontiers, and can still serve us new marvels to discover.

## IN THE BEGINNING WAS THE LYTIC PRINCIPLE

The discovery of bacteriophage has occurred on at least two independent occasions. In 1915, F.W. Twort described how, while on the search for non-pathogenic viruses of animals, he stumbled across a non-filterable material which was apparently the causative agent of "an acute infectious disease of micrococci (Twort, 1915)." He observed that micrococcus colonies could change from white to translucent, and upon this change, would cease to be propagatable. This feature was transmissible; touching a translucent colony to a white one could cause the white colony to become translucent. This transducible

phenomenon did not work on heat-killed bacteria—a living host was required. Further, such an agent of transferable bacterial disease was not isolated to the genus *Micrococcus*—Twort isolated a similar agent from intestinal bacilli that was capable of "dissolving" bacilli. In a prescient nod to the later discovery of prophages that impart virulence factors to their host, Twort even speculated on the relative toxicity of various bacteria with or without the "dissolving material" present. Yet, Twort's observations failed to generate attention, and, regrettably, two world wars interrupted his further pursuit of the matter (Adams, Mark Hancock, 1959; Stent, 1963).

Only two years later, Felix d'Herelle, a medical microbiologist, published on the discovery of an "invisible microbe" capable of not simply killing *Shigella,* but lysing these bacteria entirely (D'Herelle, 1917). Isolated from fecal samples of recovering dysentery patients, this "anti-Shiga" agent could not be cultured on its own, nor could it lyse heat-killed bacteria; rather, it was an "obligate bacteriophage"—here the term was coined, and a new field was born*. D'Herelle found that this bacteriophage could be adapted to utilize other *Shigella* strains as a host, and incorrectly speculated that this phage might prove universally adaptable to any bacterial host. This "anti-microbe" did not act as a pathogen on laboratory animals, and, in fact, could be administered to rabbits to protect against

* While this was the first report explicitly characterizing and naming bacteriophage, D'Herelle had already spent years investigating the transferable clearing phenomenon. To develop a natural insecticide for locusts—using a causative agent of grasshopper diarrheal disease, *Coccobacillus acridiorum*—he passaged bacteria through many hosts to increase virulence for a more effective pesticide (D'Herelle, 1911). As part of this process, *Coccobacillus*-infected locust feces was routinely collected, filtered, and plated onto agar. As grasshoppers recovered from disease, the bacteria recovered from their waste began taking on a new plating phenotype. Isolated colonies now displayed ragged edges, and when growth was confluent, plaques appeared, indicating that some clearing agent was present. There was no known explanation for the observed clearing, and d'Herelle's best guess was that the clearing was caused by an organism associated with *Coccobacillus,* and that this organism was the true pathogen which caused the diarrheal disease of locusts. In an aside that resounds in the heart of every grad student, d'Herelle remarks, "[i]ndeed, it must be added that for a very long time this hypothesis led me to perform many useless experiments. (D'Herelle, 1926)"

Shigellosis. The potential to deploy phage as a therapeutic antimicrobial was immediately obvious, and d'Herelle devoted much of his scientific career to this pursuit (Adams, Mark Hancock, 1959). In this pre-antibiotic era, phage therapy research was widely popular and lytic phages against bacteria that cause many of humanity's ills were discovered. Nevertheless, with perhaps the exception of phage therapy for cholera, these endeavors were unfortunately largely fruitless (Stent, 1963).

Yet, phage research was not solely devoted to its therapeutic potential—much work was put into understanding the fundamental biology of the phage. And, though fervor for phage as an antimicrobial would die down in the 1930s, its use as a tool for understanding molecular biology had just begun. In addition to his work on phage therapy, d'Herelle endeavored to understand the nature of the phage. In his 1926 book, *The Bacteriophage and Its Behavior,* d'Herelle characterizes the phage life cycle, demarcating it into the stages we continue to use to this day: 1) attachment/adsorption; 2) multiplication; 3) lysis (D'Herelle, 1926). He conceived of the one-step growth experiment, plating serial dilutions of cells infected with phage at a low multiplicity of infection over time to prove that phages were particulate in nature. His experiment and their accompanying mathematical evaluation were so sound that he tells the reader that Albert Einstein, whom d'Herelle met during a residence at the University of Leiden, found it convincing. Yet, among microbiologists, there was much initial pushback against d'Herelle's claim that the transmissible bacterial lysis was due to a discrete pathogen of bacteria. The lytic phenomenon could also be explained by an alteration of the bacterium itself, an autolysis caused by a not-yet understood alteration. The phenomenon of lysogeny was not yet understood nor characterized, but one of its associated phenotypes—the spontaneous lysis of a culture and simultaneous resistance of the selfsame host to lysis by superinfection lent ambiguity to outcomes of phage experiments. Lysis in this case would be observed, but not transferrable, making it unbelievable that lysis was caused by an infectious agent. This led to such mistrust of d'Herelle's work that bacteriophages were initially known as the Twort-d'Herelle phenomenon, rather than by his coined term. However, two outstanding researchers, F. M. Burnet, an Australian microbiologist and Martin Schlesinger, a

Hungarian chemist, took an agnostic approach to the phenomenon, and provided critical quantitative groundwork for the emerging field of phage biology.

Burnet provided evidence that phages were not a single species, demonstrating that phages were antigenically variable, even across phages that operated against the same bacterial species. Phages, therefore, were better classified by serological cross-reactions rather than host range (F. M. Burnet, 1927). Burnet provided an explanation for phage host-specificity by proposing a pairing of phage structural protein with bacterial surface proteins analogous to the antigen-antibody pairing. Evolved bacterial resistance to phage infection, therefore, could be explained by some hereditary alteration to the surface protein—bacterial extracts from sensitive bacteria inactivated phage; bacterial extracts from resistant bacteria did not. One might conclude that the host's surface had been altered, and was no longer capable of binding phage. While these concepts are presented as axiomatic in intro biology courses, to arrive at these conclusions without the aid of structural information from the yet to be invented electron microscope is remarkable. Most significantly, however, he gave a framework for understanding lysogeny that allowed it to exist in tandem with, and not contrary to, the existence of obligately lytic viruses of bacteria. Burnet found a strain of bacteria from which could be extracted a lytic principle capable of lysing a different strain of bacteria (F. Burnet & McKie, 1929). Because this isolated lytic principle had different actions according to which strain it interacted with—having no discernible effect on its parent strain, but capable of lysing a related strain—there must be an explanation to reconcile the two effects. He offered that perhaps there exists a non-infectious analogue of bacteriophage that is present in all cells in a culture, and that is part of the heritable material of a cell. This analogue might behave differently, according to the nature of the bacterium with which it is interacting, behaving as a lysogen on one hand, or inducing lysis on the other. Credibility of the bacteriophage as an entity independent of its bacterial host, was established, opening the door for the use of the phage as a model.

Schlesinger, on the other hand, used physical chemistry to understand the makeup of phage, characterizing its physical dimensions and chemical composition (Schlesinger, 1932a). His observation that phage particles are comprised primarily of DNA and protein,

in equal proportion, analogous to the hereditary portion of cells—the chromosome—would become compelling evidence for the utility of phage in understanding basic biology (Schlesinger, 1933b, 1934, 1936). His knowledge of kinetics enabled him to conjecture that phage adsorption was a process governed by Brownian motion—phage particles collide with their target as they wiggle about in random motion in the extracellular milieu (Schlesinger, 1932b). And, Schlesinger was able to utilize darkfield microscopy to visualize phage as bright puncta on a slide (Schlesinger, 1933a). This allowed him to quantify phage particles and correlate their observed count on a microscope with the number of plaques from a dilution. This critically showed that phage could be deployed quantitatively for measurable, repeatable outcomes.

Schlesinger would die prematurely in 1936, and Burnet's last work on phage was published in 1937 as he moved on to study animal viruses. Yet, the contribution of these two was imperative in establishing the phage as suitable for study through genetic, chemical, and physical means. The next leaps forward in phage biology, and indeed, in molecular biology, would come from the work of Max Delbruck and his "Phage Group" whose origins are traced in *Phage and the Origins of Molecular Biology.*

## THE PHAGE GROUP

Before the identification of DNA as the genetic material, the phenomenon of heredity presented a paradox for the physicist (Schrödinger et al., 1992). Living matter is made up of the same elements as non-living matter; a given trait, encoded by a gene, can be faithfully maintained across generations. Yet, the dimensions of a gene place it on a scale where it should be inherently unstable. The gene is composed of only a few million atoms—too small a number to exhibit orderly behavior according to statistics. Max Delbruck, a physicist, was inspired by Niels Bohr to address the seemingly irreconcilable relationship between physics and biology (Hayes, William, 1982). Delbruck published a proposed a model of the gene that relied on quantum mechanics to explain genetic

variation*. He shortly thereafter moved to Caltech to begin to experimentally probe his ideas on heredity. He met with Emory Ellis who shared his data on step-wise growth of phage (Ellis & Delbrück, 1939), and Delbruck became an enthusiastic acolyte of the bacteriophage. As Delbruck describes it, "this seemed to me just beyond my wildest dreams of doing simple experiments on something like atoms in biology" (Delbruck, 1978). The phage had found its newest, best champion as a tool for exploring biology. A flurry of discovery was to follow.

By 1940, it was widely believed that bacteria did not exhibit patterns of inheritance displayed by higher organisms. Instead, it was thought that bacteria would acquire a characteristic in response to their environment and pass on that newly acquired adaptation. In obeyance to a Lamarckian system of genetics, mutations do not preexist the environment which selects for them. In 1941, in collaboration with Salvador Luria, Delbruck addressed the concept of spontaneous versus induced mutations in bacteria using bacteriophage (Luria & Delbrück, 1943). Do phage-resistant bacteria arise because of contact with phage? Or is resistance spontaneous, arising from a change that occurs independently of phage exposure? Delbruck provided the mathematics while Luria conceived of the experiment with which to test the problem. The number of phage resistant mutants observed from plating independently grown cultures with phage would either be similar within sampling error if mutation is induced, or the number of mutants recovered from each culture would be widely variable, fluctuating far outside of the expected error. The outcome was the latter case, and one could conclude that bacterial genetic mutation is spontaneous, as in "higher" organisms, and the humble bacterium could, therefore, be a tool for exploring molecular biology. The age of bacterial genetics had come.

---

* A decade later this paper would serve as inspirational material for Erwin Schrödinger's *What is Life?* Schrödinger's little book acted as a physicist's call to arms: "From Delbruck's general picture of the hereditary substance it emerges that living matter, while not eluding the 'laws of physics' as established up to date, is likely to involve 'other laws of physics' hitherto unknown which, however, once they have been revealed will form just as integral part of this science as the former" (Schrödinger et al., 1992). Biology was the only suitable frontier for the physicist of ambition.

In 1943 the influence of Luria and Delbruck would convert Alfred Hershey to phage biology, and the nucleus of the phage group was fully formed. Yet, by this time, pursuit of phage biology was limited by the fact that independent researchers were conducting their studies using a broad range of phages and hosts, isolated from their own proverbial backyards. Experiments were not necessarily repeatable between labs, and therefore universal biological truths would be difficult to come by. Delbruck proposed the "Phage Treaty" in 1944, limiting phage work to 7 types of phage (T1, T2, T3, T4, T5, T6, and T7) that grew on *E. coli* B strains. This common set of tools would enable research to move forward in a coordinated and targeted way. These phages were chosen because they were 1) obligately lytic, avoiding the complications that lysogeny presented; and 2) consistently gave rise to distinct plaques. In 1945, the first phage meeting was organized at Cold Spring Harbor (Susman, 1995), creating a center from which to spread the spirit of collaboration married to the discipline of a quantitative and statistical approach.

Phage T2, a phage with a contractile tail and genome of around 160kbp, initially led as the darling of genetic research. T2 did not appear to exclude superinfection of T-even phages (Delbrück & Bailey, 1946), and therefore one could multiply infect bacteria with unique combinations of phage and observe the effects. Different mutants of T2 could superinfect a bacterium, and be found to recombine to generate a wild-type phage (Hershey, 1946a, 1946b). Genetic recombination was characterized to show linkage between genetic loci (Hershey & Rotman, 1948) and mathematical models to describe recombination were accurately produced (Visconti & Delbrück, 1953). In 1952, phage T2 was used to demonstrate DNA as the genetic material in the Hershey-Chase experiment (Hershey & Chase, 1952).

In 1959, phage T4 was used by Seymour Benzer to reveal the structure of the genetic material—genes were maintained in discrete, linear order (Benzer, 1959). In 1961, phage T4 was once again deployed, this time by Francis Crick, to reveal the triplet nature of the genetic code (Crick et al., 1961). That same year, R,H, Epstein found that he could isolate mutants of T4 that were capable of growing only on *E. coli* K12, but not on *E. coli* B (Epstein et al., 2012). The mutations did not map to the same locus, and some could not

grow on all strains of K12. Epstein and his group identified hundreds of such mutants that mapped to some 50 genes in T4. These conditional mutants were called ambers, in honor of a cheeky bet between Epstein and a collaborator (Edgar, 2004). The amber collection allowed for the systematic evaluation of the relationship between mutation, genetic location, and phenotype. Phage T4 dominated as the subject of choice, and a flurry of discovery followed.

In a departure from the phage treaty, gene regulation was investigated through phage lambda, and Mark Ptashne used lambda to reveal the marvelous logic of genetic circuits (Ptashne, 1967). The discovery of restriction modification systems gave insight into the immune system of bacteria (Kelly & Smith, 1970; Smith & Wilcox, 1970), but more importantly, gave a new tool with which to probe nature (Lai & Nathans, 1974)—we now possessed molecular scissors to begin to manipulate DNA on a more precise scale. Phage T7 gifted us with numerous tools---its single unit RNA polymerase and its marvelously specific and efficient promoter has become a workhorse upon which synthetic biology relies (Studier & Moffatt, 1986; Tabor & Richardson, 1985). Its DNA polymerase, which, in complex with bacterial thioredoxin, is highly processive and capable of incorporating dideoxynucleotides, was utilized as the first Sequenase for huge gains in genomic sequencing (Tabor & Richardson, 1987). And the T7 phage display system has been widely deployed for high-throughput analysis of protein-protein interactions (Deng et al., 2018). And yet, in spite of the massive contributions to biology, phage research entered a dark age between the 1970s and the early 2000s. The last Phage Course at Cold Spring Harbor took place in 1970, and the number of NIH funded grants on phage-specific research dwindled to fewer than 20 by the year 2002 (Calendar, 2006). It seemed that all there was to be known about phage was already discovered, and that what remained were minor details, of interest only to a few stalwarts for whom phage could not lose its luster.

Advances in genetic sequencing revealed that such an assessment was wrong: phage are not only abundant in the environment and found in all locations of the biosphere (Parikka et al., 2017); they also display a genetic diversity that original structural analysis could not even hint at. The majority of previously described phages were tailed

bacteriophages with double stranded DNA genomes. Yet, the first analysis of CRISPR spacer sequences in 2005 showed that only 2% of spacers had matches within known phage genomes—the remainder suggested an immense and unexplored phageome (Mojica et al., 2005). Metagenomic analysis has taken the number of ssDNA phage genomes from 56 to over 10,000 (Roux et al., 2019); the number of RNA phage genomes went from 12 to more than 15,000 (Callanan et al., 2020).

Perhaps most responsible for the renaissance in phage biology was the demonstration in 2014 that a bacterial immune system, CRISPR, could be heterologously expressed to deploy a programmable nuclease (Cong et al., 2013; Gasiunas et al., 2012; Jinek et al., 2012). Its precision and efficiency was unparalleled, and it has been subsequently used to modify genomes across all domains of life. In bacterial cells, genes cluster by function, and the sequencing revolution had shown that the amount of unknown information within defense islands—regions in the bacterial genome wherein known immune genes lie—was non-trivial (Makarova et al., 2011). Discovering and characterizing these systems against new and ever-growing libraries of phage provided by the new sequencing efforts has become the bread and butter of labs on the quest for the newest patentable molecular tool (Burstein et al., 2017; Doron et al., 2018; Millman et al., 2022).

Alongside the interest in phage for an exploitable toolbox, there is renewed interest in the fundamentals of phage biology. Advances in cryoelecton microscopy and cryoelectron tomography have allowed deeper understanding of the phage infective cycle. Some phages of *Pseudomonas* species exhibit exquisite compartmentalization during their eclipse phage: they assemble a "nucleus"—a proteinaceous assembly that protects their replicating genome, and upon which procapsids dock for packaging (Chaikeeratisak et al., 2017). Subsequently, assembled virions localize into "bouquets," revealing a spatial coordination of molecular events previously unimagined in prokaryotes (Chaikeeratisak et al., 2022). The adsorption and DNA ejection process of tailed phages has been visualized to unprecedented resolution, imparting new insights into the process that reveal new relationships between host and virus that had never even been imagined(Hu et al., 2013).

It is this final aspect on which my graduate study has focused. Bacteriophage T7, the workhorse of synthetic biology, through the lens of cryoET, has shown a new facet of its well-studied life cycle.

## PHAGE T7

Under the new taxonomy of the International Committee on Taxonomy of Viruses, bacteriophage T7 is known as *Teseptimavirus T7.* By convention, we will refer to it simply as T7. T7 is an obligately lytic virus of *E. coli*, from the original T-series of viruses described by Demerec and Fano (Demerec & Fano, 1945). It has an icosahedral capsid about 60 nm in diameter, filled with 39,937 bp of double-stranded DNA packed to a near crystalline density of 500 mg/mL (Stroud et al., 1981). Along one of these strands is the coding sequence for the 56 known genes of T7; at each end of the genome is a 160 base pair direct repeat (Dunn et al., 1983). This DNA is spooled coaxially about a proteinaceous core 26 nm long by 21 nm wide (Cerritelli et al., 1997). This core is comprised of essential proteins stacked in concentric rings—4 copies of gp16, 8 of gp15, and 10 of gp14 (Kemp et al., 2005; Serwer, 1976). From the core emanates the short, stubby tail composed of gp 11 and gp12—23 nm long, it tapers from 21 nm wide at the gp8 connector to 9 nm wide at its distal end (A. Steven & Trus, 1986). Six tail fibers radiate out from the top of the tail, each a trimer of parallel gp17 molecules (A. C. Steven et al., 1988).

As T7 moves about in the extracellular space, the virion is battered about in Brownian motion. Its tail fibers stochastically bind to the capsid, in an all-up formation that makes the virion appear as a streamlined icosohedron, or they randomly point downward, probing the environment for their targeted receptor. When in close enough proximity to its *E. coli* host, the phage will use those tail fibers to explore the bacterial surface, moving in a random walk with some fibers up and some fibers down, dynamically and transiently bound to LPS until its target receptor is found. Upon binding to this primary receptor, all six tail fibers lock into the downward position, placing the phage perpendicular to its host's surface. Perfectly poised to begin infection, the phage ejects its core proteins to irreversibly adsorb and initiate its takeover of the host. The core proteins will exit the phage head

through the portal to form an extended tail that allows the safe passage of DNA from the capsid into the cytoplasm of the bacterial host. Gp14 leaves first, extending the phage tail across the outer membrane. Gp16 is perhaps next to follow, leading with its peptidoglycan-hydrolyzing N-terminus, paving the way for gp15 behind it. Gp15 and gp16 form a complex that spans across the periplasm, with gp16 forming the cytoplasmic face of the extended tail complex (Chang et al., 2010).

**DNA EJECTION**

The phage T7 genome exhibits a polarity, with the designated left end being the first to enter the cell, the first to be transcribed, and serving as the starting point for replication (Pao & Speyer, 1973). Entry of the T7 genome into its host cell is a multi-step process, carefully timed. About 1,000 base pairs of DNA will enter the cell, exposing three strong promoters for *E. coli* RNA polymerase. These promoters can affect the rate of entry; deletion of A2 and A3 can increase the rate of entry (S. k. Zavriev & Shemyakin, 1981). In the absence of transcription, there is a block to DNA entry that is only relieved in the presence of transcription (S. K. Zavriev & Shemyakin, 1982; S. K. Zavriev & Vorob'ev, n.d.). In the absence of transcription, genome entry will arrest at 1,000 base pairs, with some proportion of DNA only entering rarely, with multiple, stochastic stops as the genome slowly and inefficiently ekes in over the course of hours (Struthers-Schlinke et al., 2000b). If *E. coli* RNAP is recruited, however, this enzyme proceeds to transcribe the next 7,000 bp at a rate of about 40 bp/s (García & Molineux, 1995b). A terminator sequence downstream of gp 1.3 will stop most transcribing complexes of *Ec*RNAP, and defines the end of class I genes (Dunn & Studier, 1980; Simon & Studier, 1973); however, there is sufficient read-through that in the absence of translation, host RNAP is capable of driving entry of the full phage genome (Kiefer et al., 1977; Millette et al., 1970). In a normal infection, though, host RNAP transcribes gene 1, T7 RNAP, and upon translation, T7 RNAP will internalize the remainder of the genome at a rate of 200-300 bp/s (García & Molineux, 1995b).

Between 8 to 12 minutes post-infection at 30˚C, the entirety of the phage genome has at last entered the cell. This process has consumed 40% of the phage's 30 minute life cycle. Contrast this with the fast entry of the lambda or T4 genome, which both enter within one minute though they lyse their hosts in 30 minutes at 37˚C, and this rate of entry seems deliberate—but to what purpose? It's been conjectured that this slow rate of entry is to allow for the transcription of phage defense genes ahead of exposure of the vulnerable portion of the genome. The first gene to be transcribed, gp 0.3, is ocr, a B-DNA mimic that potently binds to type I host restriction enzymes, inactivating them in a stoichiometric manner (Krüger & Schroeder, 1981). This protein is produced abundantly and well ahead of the entry of sites on the T7 genome that would be recognized by type I restriction proteins. Thus, protection of T7 from restriction or modification is ensured.

Yet curiously, if ocr is knocked out and phage infects a restriction-competent host, degradation of the phage genome is asynchronous with exposure of restriction sites. (Moffatt & Studier, 1988). In a wild-type infection, transcript of ocr is detectible within two minutes post-infection at 30˚C; the transcript for ocr is ~900 bp from the genetic left end. If Type I restriction recognition sites are added to 836 bp from the left end of the genome, and ocr is knocked out, then although the leading end of the genome, and thus the Type I recognition site, has presumably entered the cell by 2 minutes post-infection, degradation of the invading genome does not occur until 6 minutes post-infection. This same pattern of delay between recognition site exposure and DNA degradation is exhibited when T7 infects cells harboring the prophage P1, which encodes for a type III restriction enzyme, EcoP1, against which T7 possesses no defense. There are 24 recognition sites for the EcoP1 endonuclease within class I genes of T7, and yet the protein product of these early genes appear on a P1 lysogen host at the same time they appear on a WT host. It is not until 6-7 minutes post-infection that the phage genome becomes degraded by EcoP1, though the restriction sites had entered the cytoplasm. This protection is not conferred by the processes of transcription or translation; addition of rifampin, an inhibitor of host RNAP or chloramphenicol, which binds to the A-site of the ribosome, preventing translation, does not affect the mismatched timing of entrance of a vulnerable genetic locus

and cleavage by restriction enzyme. The mechanism by which T7 protects the leading end of its genome from enzymatic degradation but allows it to be accessible to *Ec*RNAP is still unknown. (Incidentally, this same uncharacterized mechanism by which the genome is only available to interaction with RNAP means that the genome entry assay I use, which relies on DNA methylation of GATC sites by *E. coli* DNA adenine methyltransferase (*Eco*DAM) will not show apparent DNA entry until at least five minutes post-infection.)

An alternative or additional explanation for the slow rate of T7 DNA entry is that it is a strategy for control of gene expression. Class I genes, the early genes which establish favorable conditions for phage infection within a cell, are all within the leftmost 19% of the genome. They are transcribed by host RNAP from 2 to 6 minutes post-infection at 30˚C (Studier, 1972)—their continued transcription is inhibited by the action of gp0.7 and gp2 (Nechaev & Severinov, 1999; Zillig et al., 1975). Class II genes (the middle genes which direct DNA metabolism) and class III genes (the late genes which are responsible for DNA packaging, virion assembly, and lysis) are transcribed by T7 RNAP. Class II genes are between 15% and 46% from the left end and are transcribed between 5 – 15 minutes post-infection (Studier, 1972). The promoters for class II genes are not as strong as those of class III, but their transcription continues until gp3.5 (lysozyme) inhibits T7 RNAP, effectively grinding class II promoters to a halt. Class III genes lie between 46.7% and 99% from the LE, and are transcribed from 7 minutes post-infection through lysis, which occurs at around 25 minutes post-infection at 30˚C. However, surprisingly, when T7 DNA is packaged into a lambda phage head, directing full DNA entry within two minutes post-infection (García & Molineux, 1995b, 1999), gene expression patterns remain consistent with that observed in a wild-type infection in terms of timing and dosage. Though both class II and class III promoters are simultaneously available to T7 RNAP, the strong late promoters do not preclude T7 RNAP from driving transcription from the middle class promoters.

Though a defining characteristic of phage T7 is its use of RNAP to drive genome entry, and a block to genome entry exists that is only relieved in the presence of transcription, a number of mutants of T7 capable of transcription-independent DNA entry

have been isolated and characterized (García & Molineux, 1996; Struthers-Schlinke et al., 2000b). These mutants all allow entrance of phage DNA at about the same rate: ~70 bp/s at 30˚C. They are all isolated to a 380 bp region of gene 16, but the 28 mutants characterized exhibit no obvious pattern to help explain the mechanism by which the block on DNA entry has been relieved. A single amino acid change in this region, sometimes from polar to non-polar, basic to acidic, charged to uncharged, or any in the reverse, is sufficient to lift the block. There is not well-resolved structural data of gene 16 *in situ* that would allow for accurate mapping of how those changes affect the assembled translocation apparatus (there was a high resolution structure of the apparatus published in 2021, but it was unfortunately modeled using incorrect baseline assumptions). The transcription-independent mutants display a rate of DNA entry that is temperature-dependent, and when plotted, fits the Arrhenius equation: transcription-independent DNA entry behaves as if driven by an enzyme (Kemp et al., 2004). We do not yet understand what the energy source for transcription-independent DNA entry is.

That phage genome entry requires an energy source is not self-evident. However, the second and third stages of T7 DNA entry are facilitated by the process of transcription—DNA is pulled into a cell as an RNAP advances upon its template, coupling the energy from NTP hydrolysis into translocation of DNA. It stands to reason that T7 transcription independent DNA entry requires an energy source. Most other phages do not use transcription to drive DNA entry; how do they facilitate DNA ejection? Other tailed phages have been shown to cause the transient leakage of ions upon adsorption (Daugelavicius et al., 1997; Jakutytė et al., 2012; Kuhn & Kellenberger, 1985; Letellier et al., 1999). In the case of T5, this leakage has been observed only to occur during the process of genome translocation. This coincidence of events could mean ion leakage is coupled to genome transport to drive it, or it could simply reflect that the process of DNA entry necessarily requires the formation of a pore through the bacterial cell envelope to allow DNA egress from the phage capsid. If this pore of the DNA transfer apparatus is wider than B form DNA, then as the pore opens to accommodate DNA entry into the cell, ions could freely move outside the cell, down their concentration gradients, through this newly

available channel. In support of the latter idea, phage SPP1 DNA entry can be uncoupled from membrane depolarization, and phage PRD1 DNA delivery is accompanied by an efflux of $K^+$ without membrane depolarization (Daugelavicius et al., 1997; Jakutytė et al., 2012).

Where, then, does the energy for DNA translocation come from for these phages that do not recruit polymerases to do the work? A general explanation remains elusive, but for T7, at least, we know that in the absence of transcription, the proton motive force (PMF) is required to allow DNA entry of transcription independent mutants (Kemp et al., 2004). When these mutants are treated with rifampin to inhibit host RNAP, and FCCP to collapse the PMF by allowing protons to freely cross the cellular membrane, then DNA entry arrests. Curiously, if the PMF is collapsed, but RNAP is not inhibited with antibiotics, DNA entry occurs only slowly, shifting from a pace of 40 bp/s to 6 bp/s, implying that the role of the PMF is not limited to the transcription-independent step of genome entry, but rather takes part in the overall process.

The proton motive force represents the energetic state of a bacterial membrane. It is comprised of two terms: the membrane potential (electric, $\Delta\,\psi$), and the pH gradient (chemical, $\Delta$pH). The PMF is used by bacteria as an energy source to drive ATP synthesis by the $F_1F_O$ ATP synthase (Maloney et al., 1974), motion of the flagellum (Manson et al., 1977), and substrate extrusion through the various secretion systems (Paul et al., 2008). All these processes depend upon rotation of a molecular motor, whose movements are generated through a flow of protons. This proton flow is maintained through routine metabolic activity: as part of the electron transport chain, enzymes at the cytoplasmic membrane extrude protons outward to generate a gradient wherein the concentration of protons in the periplasm exceeds the concentration of protons in the cytoplasm. The only route for a $H^+$ to travel down this gradient and return to the cytoplasm is through specific membrane-bound structures, such as those found within the $F_O$ portion of ATP synthase (Klusch et al., 2017; Suzuki et al., 2002) or the MotA/MotB portion of the flagellum (Takekawa et al., 2016). Proton flow through these channels can be modified based on environmental conditions—for example, ATP synthase can function in the reverse

direction depending on the metabolic state of the cell, catalyzing the synthesis of ATP in one direction, or hydrolyzing it in the other (Maloney et al., 1974).

Does there perhaps exist a proton channel within the translocation apparatus of T7 that allows a coupling of proton transport with genome entry? Is the PMF requirement of T7 transcription independent DNA entry a hint that this apparatus is a molecular motor, pairing proton flow with dynamic movement analogous to the flagellum or Type III secretion system? Adding to the intrigue is the observation through cryoET that ATP synthase is recruited to the cytoplasmic face of phage T7's DNA translocation apparatus. ATP synthase forms a hexameric ring, surrounding the exit channel of the phage's extended tail. What purpose does this structure serve? A non-invasive assay will be used to investigate the role of ATP synthase in phage T7 DNA entry.

# CHAPTER 2: T7 DNA REPLICATION REVISITED

## INTRODUCTION

Bacteriophage T7 has a linear genome 39,937 base pairs in length (Dunn et al., 1983). It enters its host cell in a conserved, polar fashion, from the genetic left end to the genetic right end (Pao & Speyer, 1973). While some double-stranded DNA phages will circularize their genomes upon entry (Hershey et al., 1963) to protect their ends from degradation by host exonucleases and to facilitate faithful replication of the genetic material, T7 opts not to. Rather, T7 DNA persists in linear form through the entirety of its life cycle. Linear chromosomes must have a mechanism for dealing with the end replication problem; how T7 precisely does this remains an open question.

At around 10-12 minutes post-infection—immediately following the complete transcription driven entry of the genome (García & Molineux, 1995b), phage DNA replication begins (Studier, 1969). The T7 origin of replication is located 5,921 bps from the genetic left end, near tandem RNA polymerase promoters (Dressler et al., 1972; Rabkin & Richardson, 1988; Saito et al., 1980), and transcription by T7 RNAP is required for replication to initiate (Fuller & Richardson, 1985; Hinkle, 1980; Romano et al., 1981). Newly assembled phage genomes will be almost exclusively comprised of nucleotides harvested from the host (Labaw, 1951, 1953; Siddiqi et al., 1952), whose genome is completely degraded by gp3 and gp6, T7's endo- and exo- nucleases, respectively, from 7 to 15 minutes post-infection (Sadowski & Kerr, 1970). Electron microscopy has shown that once the replication bubble forms on the parent strand, it expands into an eye form (Wolfson et al., 1972). The T7 DNA polymerase complex, comprised of gp5 and its processivity factor, host thioredoxin, assemble with gp4A and gp4B, the helicase primase,

to form the T7 replisome, which proceeds bidirectionally at 300 bp/s, driving the growth of the observed replication bubble (Egelman et al., 1995; Mark & Richardson, 1976; Matson & Richardson, 1985; Modrich & Richardson, 1975; Tabor & Richardson, 1981). The replication fork runs off the left end of the genome, and Y-form molecules can be detected (Dressler et al., 1972; Wolfson et al., 1972). The next steps in the replication cycle are mechanistically obscure. A 160 bp sequence is present in two copies in the T7 genome, one located at the left end, one located at the right end. This sequence is called the terminal repeat (TR). After the first round of replication (**Fig. 2.1A**), the daughter molecules bear the hallmark of the end-replication problem of linear genomes: 3' overhangs (**Fig. 2.1B**). The TR provides a convenient mechanism for preventing the loss of genetic material from these ends: the 3' overhangs at either end of the genome are complimentary along the 160 bp sequence. They can therefore anneal to one another, incompletely replicated right end of one daughter molecule joined to incompletely replicated left end of the other daughter molecule, to form a linear concatemer of phage DNA (**Fig. 2.1C**). This region of end to end joined molecules is termed the concatemer junction (CJ). Yet, while the daughter strands may have aligned and annealed to prevent the loss of their three prime ends, there is a single terminal repeat between the two chromosomes, and the product of one round of replication is not two full-length genomes. It is uncertain if this represents a "good enough" scenario for T7: replication continues and the length of the concatemer of DNA grows (**Fig. 2.1D**). T7 replication may be wasteful, with every other daughter genome produced as less than full length, and ultimately discarded. Or, the TR may be duplicated at a later stage of phage development.

After the formation of concatemers, electron microscopy reveals the next stage in replication: extensive branched complexes of DNA, comprised of many interacting and interconnected phage genomes are observed. Homologous recombination between

replicating molecules, requiring the presence of gp3 and gp6, occurs extensively (Hori et al., 1979; Langman & Paetkau, 1978; Lee & Sadowski, 1983). Phage DNA may at this point become associated with the host cell-membrane (Center, 1973), and packaging begins. Does the packaging reaction obligately couple with replication for the formation of full length T7 genomes? Or does the packaging event dispense with every other replicated genome?

James Watson offered a popular model for T7 replication (Watson, 1972) assuming molecular waste unlikely. It proposed a way that T7 might simultaneously duplicate its TR and separate daughter strands from concatemers. A nuclease nicks DNA at flanking regions of the terminal redundancy. DNA polymerase (DNAP) can initiate synthesis at the 3' ends exposed by the nicks; DNAP procession would displace the 5' -end of the non-template strand. As the 3' ends of each nicked strand elongate, they will eventually traverse across the terminal redundancy, to the point of the initial nick. As each DNAP processes along its template, the molecules are no longer joined. While this model is pleasingly simple, fifty years of evidence demonstrate that it is unlikely to be true.

As replication proceeds past the first round, concatemers grow into complexes sufficiently large that they can be separated from unit size genomes on a sucrose gradient (Paetkau et al., 1975). If Watson's model were true, then within those separated concatemers, one might find mature left and right ends (that is, ends that are capped with the 160 bp TR) that are produced concurrently from his proposed nicking reaction. However, experimental evidence suggests that the right end and the left end form in uncoupled reactions. The mature right end (RE) forms during DNA packaging (Chung & Hinkle, 1990a)—gp18 and gp19, the small and large subunits of terminase, respectively, have sequence specificity will cleave concatemeric DNA 160 bp to the right of the CJ to form a mature right end. The mature left end (LE) forms separately—*in vitro* packaging

experiments show that in the absence of gp2, an inhibitor of *Ec* RNAP, gp5, or gp6, mature right ends form and are packaged, but the left end of the packaged genome is truncated by at least 160 bp (White & Richardson, 1987). Mature left end formation occurs through an as-yet uncharacterized manner that involves the formation of a hairpin (HP) (Chung & Hinkle, 1990b). This hairpin is formed independently of DNA packaging and appears in the absence of gp3, gp10 (the major capsid protein), and gp19. In the absence of gp10 and gp19, mature right and left ends are absent, implying that DNA packaging is required for the formation of full length, mature genomes (Chung & Hinkle, 1990a). Additionally, the hairpin is uniquely associated with concatemeric DNA; it can be observed during DNA packaging, but it is not observed in DNA isolated from fully mature phage particles. It is cleaved after the packaging reaction has completed (Kim et al., 1997)—the packaging reaction, occurs on concatemeric DNA, terminating in the cleavage of the hairpin. So, in a WT infection, a mature right end is not only found in unit length DNA, but it is also associated with concatemeric DNA. The mature left end, in contrast, is only present in full length genomes. Each mature genetic end appears to be formed by dedicated and independent processes. What does this mean for the issue of economy of replication? We offer a short experiment that may provide some insight.

## RESULTS

T7 DNA replication has been traditionally measured by pulse-labeling phage-infected cells with [$^3$H]-thymidine—host DNA synthesis has ceased by 6 minutes post-infection, so any thymidine incorporation past this point is phage-initiated. The rate of tritiated thymidine incorporation is taken as a readout of phage DNA replication. By this method, phage DNA replication begins at 8 minutes post-infection, and peaks at 15 minutes post-infection (North & Molineux, 1980)—well ahead of lysis of the host cell, which

occurs at about 25 minutes post-infection (**Fig 2.2A**). Yet, because phage T7 cleaves host DNA during infection, and incorporates the liberated nucleotides into its own genome, the pool of tritiated thymidine must compete with an abundant nucleotide pool from the host. This may render observations about DNA replication made by this method unreliable (Zhang & Studier, 2004). We therefore took a different approach in our examination of phage DNA replication.

To offer another way of observing the dynamics of T7 concatemer resolution, we isolated total DNA from phage-infected cells at various time points after infection. This DNA was digested with Dpn I to shatter the host genome, and Xmn I to cleave the phage genome into discrete fragments. **Figure 2.2B** shows the results of this experiment, with each lane representing a time post-infection. DpnI cut sites along the host genome are sufficient to render it a smear on an agarose gel, with only a few discrete bands remaining that are easily distinguished from phage DNA by size and by relative intensity. A linear map of the T7 genome with Xmn I cut sites is shown to demonstrate the correspondence of band size with loci along the phage chromosome. By 13 minutes post-infection, the background of host DNA is much diminished, reflecting the combined effect of DpnI digestion and phage nucleases. The phage genome is readily resolved and quantifiable. The magnitude of replication prevents equal loading of the gel and requires that the earliest timepoints have four times the amount of DNA loaded versus the latest timepoints. An increase in intensity of the bands of phage DNA is still readily observable. By 11 post-infection, it is clear that the relative intensity of the left end of the genome, annotated as band F, has decreased compared to its nearest neighbor, band E—replication has begun, and the mature left end will continue to decrease in relative intensity for some time as concatemers form and lengthen. At 13 minutes post-infection, the CJ appears, noted with a red arrow—at least one round of replication has completed and at fifteen minutes post-

infection, the HP, noted with a blue arrow, can be observed, signaling that maturation of the left end has begun.

To find the magnitude of the increase in DNA during replication, the relative amount of phage DNA within a cell was quantified by measuring the total intensity of phage bands for each lane, multiplying by the appropriate factor to account for the difference in loaded amounts, and plotting the result over time, relative to the first lane, to see how the amount of apparent DNA changed from infection onset. **Figure 2.2C** shows that the relative amount of phage DNA begins increasing by ~11 minutes post-infection and continues to accumulate as infection proceeds. T7 DNAP proceeds at a rate of 300 bp/s and a set of replisomes should take 2.5 minutes to complete one round of replication—thus, the detected onset of replication via gel at 11 minutes post-infection and the appearance of the CJ on the gel at 13 minutes post-infection align well with this rate.

The relative amount of mature genetic left ends were calculated as a ratio of the intensity of band F divided by the intensity of band closest in size to it, band E. This ratio was plotted versus time, to show that the relative amount of LE increases sharply at 10 minutes post-infection **(Fig 2.3A)**, as replication initiates at this region of the genome. The relative amount of LE thereafter decreases as concatemers form and the LE is sequestered in the concatemer junction. By about 17-18 minutes post-infection, the amount of LE begins to increase, as genomes are fully packaged into phage heads, resulting in formation of mature left ends. This is in agreement with the rise observed on a one-step growth curve, where the eclipse period ceases and new virions can be detected. The relative amount of LE does not return to the baseline observed at early infection, before DNA replication began. This suggests that not all concatemers are processed and packaged, which must be true if DNA replication continues until lysis.

The relative amount of the mature genetic right end (RE) was calculated by dividing the intensity of the RE, annotated as band J, by the intensity of the band nearest in molecular weight, band K. This calculated amount was plotted over time **(Fig 2.3B)**, and the relative amount of RE is virtually unchanged until 12 minutes post-infection, when it drops, as it, like the LE, is sequestered in the concatemer junction. At 15 minutes post-infection, the relative amount of the RE experiences a slight rise; the event that initiates mature right end formation begins. Again, similarly to the LE, the relative amount of the RE, while increasing through late replication, does not recover to initial levels observed, suggesting some waste of replicated genetic material.

To give some insight into how much mature phage DNA is made compared to what is replicated, the ratio of intensity of the CJ band over the intensity of the LE band was plotted over time (**Fig 2.3C**). Upon its appearance at the completion of the first round of replication at 13 minutes post-infection, the proportion of CJ to LE increases. At ~16 minutes post-infection however, this proportion begins to fall, signaling that packaging on concatemers has begun. By the end of the time course, at 40 minutes post-infection, when cell lysis has already occurred, the CJ/LE is ~0.8—over 40% of recoverable phage DNA is in concatemers. Phage DNA replication is indeed wasteful.

To understand more about the timing of left end maturation, the ratio of HP to LE was plotted over time **(Fig 2.3D)**. As visualized with this assay the HP appears at 15 minutes post-infection, concurrent with the usual onset of phage DNA packaging. The HP is cleaved at the termination of packaging, and the relative abundance of the hairpin only decreases over time, suggesting that whatever initiates its formation is outpaced by the rate of the action of the packaging event. The decrease in relative amount of HP continues through the course of infection, through lysis.

## DISCUSSION

This gel-based assay for replication allows insight into the major events during phage DNA replication. While [$^3$H]-thymidine incorporation has been used to measure the rate of DNA replication, the radio-labeled nucleotide pool is not sufficient to compete with the abundant nucleotide pool provided by the phage-shattered host genome. [$^3$H]-thymidine incorporation peaks at 15 minutes post-infection and precipitously declines, implying shut off of DNA replication well before host cell lysis occurs. In contrast, the gel-based assay offered here shows that DNA replication, once begun, continues until host cells lyse. Via this assay, there does not appear to be a shut off event for replication. However, this assay cannot compete with the sensitivity of radio-labeled nucleotides—replication onset via [$^3$H]-thymidine incorporation occurs at 8 minutes post-infection. Via this gel-based method, an increase in DNA is not detectable until two minutes later. Mature genetic ends were observed to change in relative abundance during infection, variously increasing during the first round or rounds of replication, decreasing as concatemers formed and ends became sequestered, and then increasing once more as mature ends form during concatemer processing and packaging. And while specific events during infection lead to mature left end and right end formation, by the end of infection, not all replicated DNA has mature ends. About 40% of replicated DNA remains in concatemers---DNA replication occurs in excess, though the relative amount of discarded genetic material is still an open question.

## MATERIALS AND METHODS

### Bacteria, Phage, and Media:

IJ2011, an *E. coli* BW25113 strain from the Molineux collection was used as the wild-type host for all infections. Cells were grown in a shaking water bath at 30˚C, in LB supplemented with 0.4% glucose, and buffered with 40 mM MOPS pH 7.0. The WT T7 strain used is a long-term resident of the Molineux lab, deposited in the ATCC as BAA-1025-B2. Phages were propagated and subsequently purified on a CsCl gradient, as historically described (Studier, 1969). Titers were determined by plaque assay, and phage stock was stored at 4˚C and used for a maximum of two weeks, after which timepoint stocks lose synchronicity of infection.

### DNA Replication Assay:

Bacteria were grown to a density of 2 x $10^8$ cells/mL in the conditions noted above. Cells were then infected with T7 at a multiplicity of infection of 5. To stop all cellular processes and harvest all DNA, we utilized the method outlined by Paetkau et al (Paetkau et al., 1975). At defined intervals post-infection, 750 μL of infected cells were added to an equal volume of ice-cold killing solution (75% EtOH; 2% phenol; 20 mM NaAcetate, pH 5.3; 8 mM EDTA pH 8.0; 15 mM NaOH), vortexed for 10 seconds, and placed on ice for the duration of the infection. Subsequently, samples were spun down centrifuged at 13K RPM for 5 minutes to pellet DNA and other cellular debris. The supernatant was discarded, and the samples were either immediately processed, or stored at -20˚C to await processing.

Samples were then gently resuspended in 500 μL of TES (50 mM Tris-hydrochloride, pH 8.0; 25 mM EDTA; 50 mM NaCl) containing 0.5% SDS and 50

μg/mL Proteinase K. Proteinase K digestion was carried out at 55˚C for one hour, and 200 μL phenol equilibrated to pH 8 was added to remove protein and Proteinase K from the solution. RnaseA was added at 0.2 mg/mL and RNA was digested for one hour at 37˚C. Two rounds of phenol/chloroform/isoamyl alcohol treatment followed for clean-up, and DNA was ethanol precipitated and resuspended in 50 μL $H_2O$.

25 μL of DNA from each time point was digested with Xmn I and Dpn I (NEB Labs) according to NEB protocols. The magnitude of replication over time is such that lanes cannot be equally loaded with digested DNA without obscuring the results of early timepoints. Therefore, lanes were loaded as follows: lanes 1-4, 20 μL DNA; lanes 5-8, 10 μL DNA; lanes 8-16, 5 μL DNA. Digests were run on a 1% agarose gel at 20V for 10 hours. Gels were stained for 30 minutes with 1:1000 dilutions of SYBR Gold in TBE buffer, prepared according to Cold Spring Harbor protocols ("TBE Buffer," 2006), and DNA was imaged on the Typhoon 9500. Images were labeled and quantified using ImageJ (Schneider et al., 2012) and GelAnalyzer 19.1 (Lazar, Jr & Lazar, Sr, n.d.).

**Analysis of DNA:**

All experiments were done in triplicate and data was analyzed and visualized with R (R Core Team, 2021), run on RStudio (RStudio Team, 2022) with the packages dplyr, ggforce, ggplot2, scales, and tidyr. Figures were created using BioRender (BioRender.com).

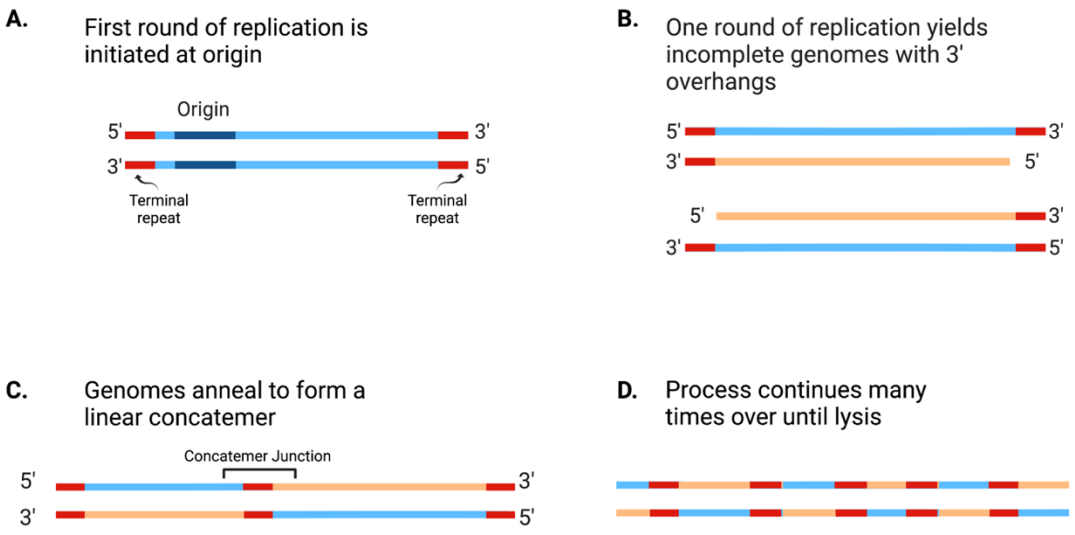


**Figure 2.1**. A model for T7 concatemer formation:

(A) Phage DNA replication is initiated near the left end of its linear genome. (B) The first round of replication leaves each daughter strand with 3'-overhangs on the lagging strand and incomplete sets of genetic information. The 3'-overhangs are complementary across the 160 bp terminal repetition (TR). (C) The daughter strands can anneal across the complementary region to form a concatemer. This does not give rise to mature progeny genomes; a single TR is present between genomes. The region where genomes are fused incomplete end to incomplete end is termed the concatemer junction (CJ) (D) This process continues through replication, giving rise to long concatemers that will homologously recombine at a later stage, forming high molecular weight, complex DNA molecules that must be processed before DNA packaging.

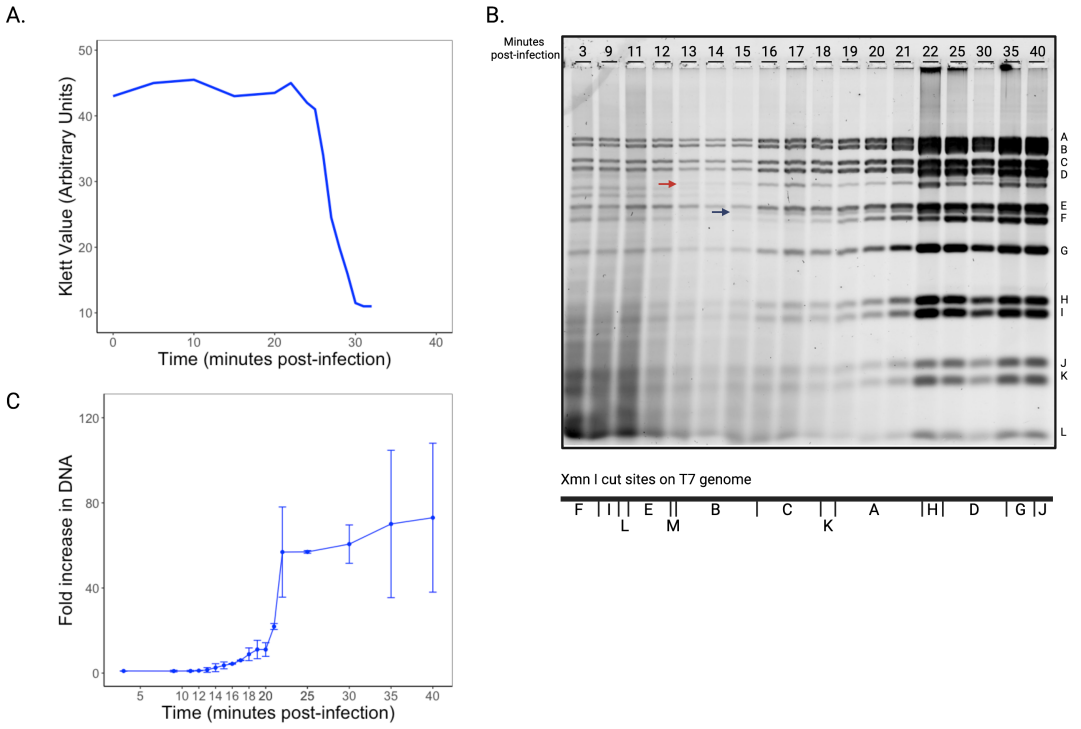


**Figure 2.2**. A direct comparison of methods for assaying *in vivo* DNA replication

T7 infection was initiated on cells at a density of $2x10^8$ cells/mL. (A) Lysis curve of infected cells. The optical density of a phage-infected culture (MOI 5-10) was plotted over time. Lysis begins ~25 minutes post-infection. (B) An agarose gel showing cut phage DNA over the duration of infection. Cells growing in LB-0.4% glucose, 40 mM MOPS pH 7.0 were infected with phage at an MOI of 5. At indicated times post-infection, samples were removed and mixed with equal volumes of a cell-killing solution. Total DNA was extracted, digested with Dpn I and Xmn I, and run on a 1% agarose gel. Gels were stained with SYBR gold and imaged. Lanes are not equally loaded: minutes 13-16 have half as much loaded sample as minute 3; 17-20 have ¼ the volume of minute 3; minutes 21-40 have 1/8 the volume of minute 3. The red arrow indicates the concatemer junction, while the blue arrow indicates the hair pin. Below the gel is a map of the T7 genome showing Xmn I cut sites. These are labeled and labels correspond to

bands seen on the agarose gel. (C) The fold increase in phage DNA over time. Total intensity of phage-specific bands was tallied for each lane and then plotted to visualize replication over time.

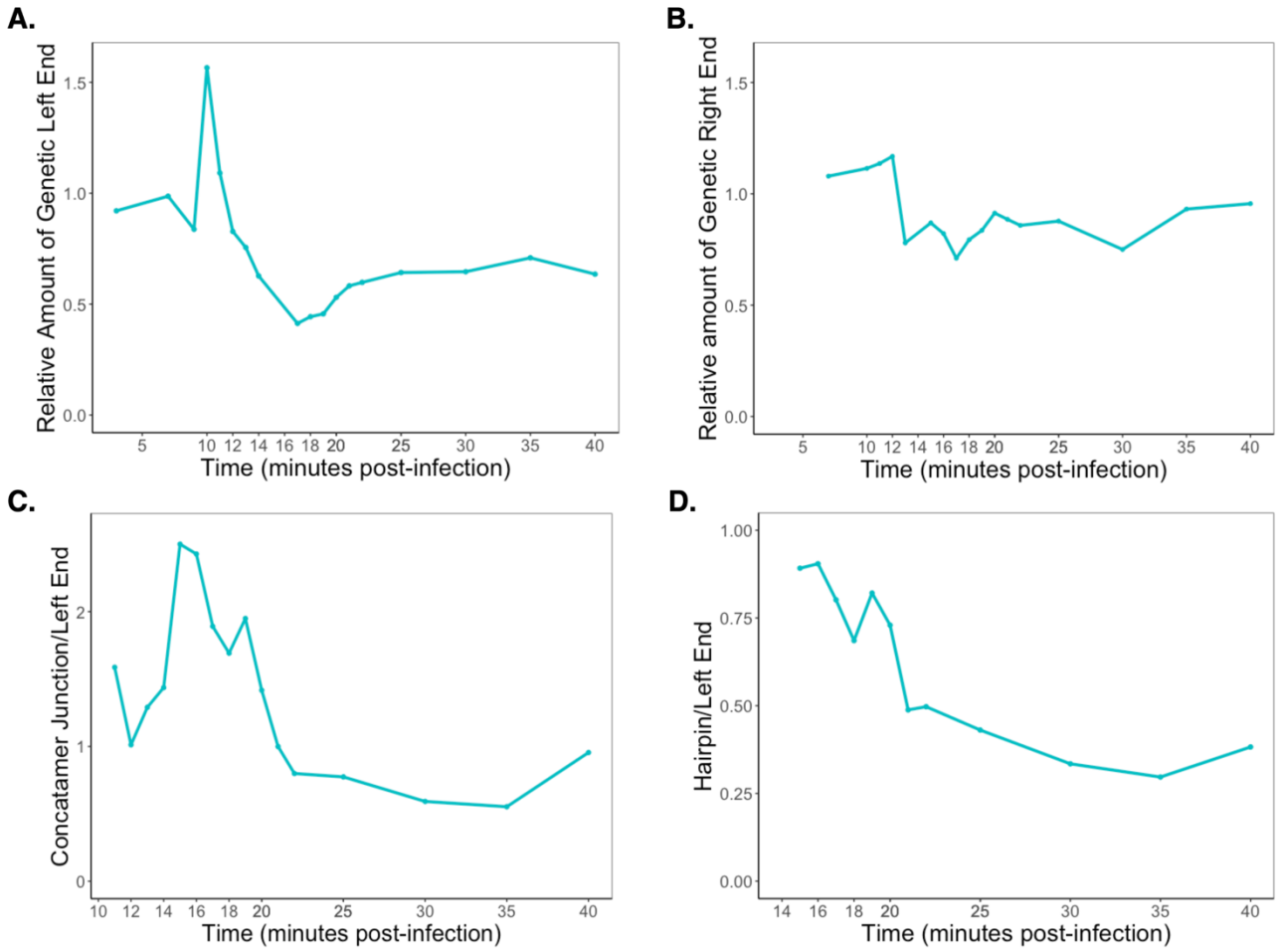


**Figure 2.3**. Mature genetic ends change in relative abundance during replication, never recovering to their original proportions:

Cells were infected at a density of $2x10^8$ cells/mL with phage T7 at an MOI of 5. An assay for replication was carried out as detailed in methods. Data shown is an average of three biological replicates. **A.** Quantification of the relative amount of the mature T7 genetic left end over time. The intensity of the band representing the mature left end was divided by the intensity of the band nearest to it in molecular weight, and this value was plotted over time. T7 origin of replication is located at the genetic left end, and this region is the first to increase in relative abundance before falling as ends are sequestered

in concatemers. **B.** The relative amount of the genetic right end over time. The intensity of the band representing the RE was divided by the intensity of the band nearest to it in molecular weight, and this value was plotted over time. The amount of RE rises at replication onset and experiences a decrease in relative abundance similar to the left end. **C.** The concatemer junction over time. For each timepoint, the intensity of the CJ band was divided by the intensity of the LE band, and this value was plotted. The CJ appears after the first round of replication, increasing in abundance relative to the left end, before dropping as packaging initiates. **D.** The relative amount of hairpin over time. For each timepoint, the intensity of the HP band was divided by the intensity of the LE band, and this value was plotted over time. The HP appears at fifteen minutes post-infection and decreases over time until host cell lysis.

# CHAPTER 3: PHAGE T7 GENOME ENTRY INVOLVES HOST ATP SYNTHASE

**Acknowledgements:** The cryo-electron tomography observations shared in Figure 1, and upon which this chapter hinges were the work of former members of the Jun Liu lab, at the Yale University School of Medicine, in New Haven, CT and at the McGovern Medical School at The University of Texas Health Science Center in Houston, TX.

In 1952, the Hershey-Chase experiment demonstrated that tailed bacteriophages eject DNA into their host cells. More than 70 years later, the driving force for this event remains uncertain. However, cryoET has offered new insight into this long-studied process, and introduced a previously unknown component of the T7 DNA translocation channel: *E. coli* ATP synthase. The energy source of genome ejection has been a point long debated. Here we offer evidence that bacteriophage T7, which is known to drive a portion of DNA ejection via transcription, recruits ATP synthase to harness the proton motive force to aid DNA ejection.

## INTRODUCTION

To successfully initiate infection, bacteriophages must deliver their DNA into a host cell. This requires the hydrophilic DNA molecule to traverse a hydrophobic cell membrane. Further, for phages that infect a gram-negative host, this barrier is tripartite: outer membrane, periplasm, and inner membrane that together span up to 40 nm. Phage T7 is a short-tailed lytic *Podovirus* that infects *E. coli.* Its external tail extends 23 nm from the baseplate, and is thus insufficient to traverse the gram-negative cell envelope(A. Steven & Trus, 1986). Biochemical assays showed that T7 ejects core proteins gp 14, gp 15, and gp 16 from its capsid through the tip of its tail and that these proteins are cell-envelope associated; it was predicted that these proteins form a channel across which the genome can safely cross the cell-envelope(Chang et al., 2010; Serwer et al., 2008; Struthers-Schlinke et al., 2000a). Cryo-electron tomography (cryoET) has given us profound insight into the dynamics of early phage infection, allowing confirmation of the biochemistry-based hypothesis: the core proteins form a channel for phage DNA delivery(Hu et al., 2013). However, this same study revealed a new unknown in phage T7 infection.

The appearance of the trans-envelope channel coincided with the appearance of a 30 by 60 nm toroidal structure at the cytoplasmic interface of the channel. The electron density of this structure could not be accounted for by any protein found within the phage capsid, but its initial appearance was too low resolution for identification. To understand the nature of this structure, and its role in the T7 infection process, higher resolution images were obtained, and we then examined T7 growth and rates of DNA entry with and without the structure present. The cryoET experiments identified the new cytoplasmic component of the translocation channel as *E. coli* ATP synthase. We found defects in both phage lysis of host cells as well as in phage DNA entry in the absence of ATP synthase at non-neutral pH. Phage DNA entry could be hastened by an induced influx of protons, only when ATP synthase was present and the phage-intrinsic brake on DNA egress was removed. The discovery of ATP synthase as a subunit of the T7 DNA translocon, and the pH-dependent alteration of the rate of phage DNA entry makes for the intriguing possibility that the T7 DNA translocon is rotary motor, analogous to the bacterial flagellum and secretion systems.

## RESULTS

To define the composition of the previously reported toroid, the early steps of T7's infective cycle were visualized by cryo-electron tomography. CryoET requires samples less than 500 nm thick—*E. coli* mini cells(Liu et al., 2012), were therefore used as hosts for T7 infection. 3D reconstructions showed a subclass of adsorbed virions at an intermediate stage of infection: the internal core proteins are ejected from the capsid to form a transenvelope channel, the capsid remains electron dense with DNA, and the enigmatic structure, 30 nm in diameter, at the cytoplasmic face of the inner membrane, coaxial with the trans-envelope channel, was apparent (**Fig. 3.1A**). To generate an averaged

structure of high-resolution, particles were selected, unveiling the unidentified structure to be comprised of the $F_1F_O$ ATP synthase: the structure appeared when T7 infected WT mini-cell hosts (**Fig. 3.1B**); when T7 infected Δatp mini-cell hosts, no density was visible below the cytoplasmic membrane (**Fig. 3.1C**). After refinement, a central slice through the translocation channel shows that multiples of ATP synthase are organized around the translocation channel (**Fig. 3.1D**) arrayed in a hexameric ring with a central pore ~4nm in diameter (**Fig. 3.1E**). The appearance of the ATP synthase hexamer is coincident with the appearance of the DNA translocation channel: it is only visible in the fraction of adsorbed particles that feature the tail extension across the cell envelope. In the fraction of adsorbed particles with empty phage heads representing virions that have fully ejected DNA, the translocation channel is gone, along with the hexameric ring of ATP synthase. A slice of an averaged structure of a single ATP synthase from the base of the translocation apparatus shows the full ATP synthase complex is apparently recruited (**Fig. 3.1F**). The $F_1$ cytoplasmic portion and the stator are readily discernible, and the atomic structure of *E. coli* ATP synthase can be easily docked into the CryoET density (**Fig. 3.1G**).

The coincidental appearance of a hexamer of ATP synthase with the formation of T7's DNA translocation channel suggests a possible relationship between ATP synthase and genome delivery. T7's method of DNA entry is distinct from that of both phage lambda, representative member of the long, flexible-tailed *Siphoviridae*, and phage T4, a member of the contractile-tailed *Myoviridae.* To determine if ATP synthase plays a distinct role for DNA delivery of T7, one step growth curves, which give insight to the overall dynamics of phage infection, on either a WT or Δatp host were carried out for phage lambda, phage T4, and phage T7 (**Fig. 3.2A)**. The latent periods of all three phages are unchanged by growth on an ATP synthase deficient host. Lambda and T4 show consistently reduced burst sizes on Δatp *E. coli.* The behavior of T7, however, is too

variable to generalize. Lysis curves under more varied conditions were carried out. When T7 infects ATP synthase deficient *E. coli* at mid-log, at 30˚C, at an MOI of 5, lysis is delayed by about two minutes when cultures are grown at pH 7 or pH 8 (**Fig. 3.2B**). At pH 6.1, lysis onset is delayed by about five minutes in a Δatp host. When T7 infects Δatp *E. coli* at late mid-log (**Fig. 3.2C**), a deficiency in infection becomes more stark: at pH 6.1, infected cells do not lyse within two hours; at pH 7, the lysis delay is extended to five minutes; at pH 8, however, the delay is unaltered.

To test if ATP synthase is utilized during T7 genome ejection, we utilized a modified version of an assay pioneered in this lab to measure the rate of DNA ejection (García & Molineux, 1995b). Briefly, we measured the rate of phage genome entry by infecting *E. coli* with T7 variants that have been engineered to have multiple GATC sites distributed across their ~40,000 bp genomes. These phages were growth on hosts lacking DNA methyltransferase (Dam), and are completely unmethylated. Experiments were carried out on WT (IJ1133) or Δatp (IJ1525) hosts bearing the plasmid pTP166, which overexpresses Dam. As phage DNA enters the host cell, DNA is methylated at distinct loci. DNA was extracted at various times post-infection, cut with Dpn I, which only cleaves methylated GATC sites, and run on an agarose gel. As DNA translocation proceeds, an increasing number of GATC sites enter the cytoplasm and become methylated. The number of distinct bands formed by Dpn I cuts will increase over time, with each band corresponding to a distinct genomic region of defined size. Thus, the amount of DNA inside of the cell over time can be approximated from the appearance of bands on a gel and an estimate of the overall rate of DNA entry can be made.

T7 genome delivery is a multistep process requiring the involvement of at least three molecular machines: the phage extended tail that conducts DNA across the cell envelope (Struthers-Schlinke et al., 2000a), *Ec* RNAP (S. K. Zavriev & Shemyakin, 1982;

S. K. Zavriev & Vorob'ev, n.d.), and T7 RNAP (Moffatt & Studier, 1988) (**Fig. 3.3A)**. The major elements encoded by T7 to drive DNA entry include three strong promoters for *E. coli* RNA polymerase (*Ec* RNAP), A1, A2, and A3, which recruit *Ec* RNAP to internalize ~7,000 bp of the phage genome via transcription; gene 1, T7 RNAP, which internalizes the remainder of the ~40kb genome; and gp 16, a component of the translocation channel that can arrest genome internalization in the absence of transcription. Our functional "WT" T7 used in this experiment is designated as Dam12 (García & Molineux, 1995b) and has 12 Dpn I cut sites along its length, and is WT for the major control elements mentioned (**Fig. 3.3B** and **3.3C**). We also utilize a transcription independent T7 variant, T7 Dam12, *16I754T* (García & Molineux, 1996), here referred to as TI-T7, for convenience's sake. It contains the 12 Dpn I sites and has a single point mutation in gene 16 that allows entry of the entire genome in the absence of transcription. T7 D394-5911, Dam10 (Struthers-Schlinke et al., 2000a) is an entry-deficient T7 variant, referred to in this text as ED-T7, which has deletions of the A1, A2, A3 promoters as well as T7 RNAP, rendering it unable to enter a cell. Lastly, we also use a rescued entry-deficient T7, T7 D394-5911, Dam10, *16I754T*, referenced as RED-T7, which has the deletions of ED-T7, but contains the point mutation in gp16 that rescues its ability to deliver its DNA into a cell.

To test if ATP synthase is utilized in the overall DNA entry process, we conducted our entry experiment using Dam12, and found that there was no difference in the rate of T7 DNA entry between a WT host and a Δatp host (**Fig. 3.3D** and **3.3E)**. Based on the slope of the plotted line, the phage genome enters at an initial rate of ~60 bp/s, and at a final rate of ~200 bp/s, values in approximate agreement with the known rates of *E. coli* RNAP transcription (Condon et al., 1993; Ryals et al., 1982; Vogel & Jensen, 1994, 1997) and T7 RNAP transcription, respectively, and are of similar magnitude of previously reported findings from this lab (García & Molineux, 1995b, 1996; Kemp et al., 2004;

Struthers-Schlinke et al., 2000a). The full genome is internalized by 12 minutes post-infection for both conditions. At 30˚C, in LB buffered to pH 7, ATP synthase does not appear to affect the rate of DNA entry.

We tested if ATP synthase is involved in *Ec* RNAP-directed DNA entry by performing our entry assays on cells treated with chloramphenicol to prevent translation of gene 1, T7 RNAP. Though the host enzyme is typically only used to transport a 7kb region of the phage genome, in the absence of T7 RNAP, *Ec* RNAP will internalize the complete phage genome at a constant rate of about 40 bp/s (Struthers-Schlinke et al., 2000a). We found no difference in the rate of *Ec* RNAP-directed T7 genome translocation when the host lacked the ATP synthase operon, and the overall rate of entry was about 40 bp/s, though for both hosts, the process did not discernibly begin until ~7 minutes post-infection, and the time to completion was ~19 minutes. **(Fig. 3.4A)**.

Transcription is required for full entry of the T7 genome, and in its absence, entry will arrest after ~1,000 bp have entered the cell (García & Molineux, 1995b, 1995a). The stop signal for DNA entry has not been identified, but a single point mutation in gene 16 is sufficient to not only abolish the stop, but to allow entry of the full genome at a constant rate in the absence of transcription(García & Molineux, 1996). This transcription-independent method of entry is energy dependent: the proton motive force (PMF) is required(Kemp et al., 2004). To determine if ATP synthase is required for transcription-independent DNA entry, we performed our entry assays using RED-T7. RED-T7 cannot recruit *Ec* RNAP, nor make its own T7 RNAP, and thus the only mechanism for its DNA to enter the cell is through the gene 16 mutation—the transcription-independent method of entry. We found the rate of RED-T7 genome entry was ~54 bp/s on both WT and Δatp hosts, and full entry occurred by 15 minutes post-infection (**Fig. 3.4B**). ATP synthase is not required for transcription-independent DNA entry.

We know that gene 16 controls the amount of DNA that enters the cell—the presumed brake or clamp that halts genome translocation has been isolated to two regions within gene 16 (Struthers-Schlinke et al., 2000a). Is ATP synthase part of this system? To test if ATP synthase is required to arrest genome translocation, we performed our entry assays with ED-T7, which has no mechanism for DNA entry: it cannot recruit *Ec* RNAP, and it does not make its own. If ATP synthase is a necessary component of the braking system, then its absence will allow ED-T7 DNA ejection. We found that ED-T7 cannot eject its genome into a WT or a Δatp host, and no genome entry was detected within 60 minutes of infection (**Fig. 3.4C)**.

ATP synthase is a rotary motor (Noji et al., 1997; Zhou et al., 1997) that uses the PMF to drive ATP synthesis (Jagendorf & Uribe, 1966; Kagawa & Racker, 1971). Net inward movement of protons across the membrane-embedded $F_O$ portion of this nanomachine causes the rotation of the cytoplasmic $F_1$ portion. The mechanical energy from rotation is used to catalyze the formation of ATP from ADP and inorganic phosphate. This reaction is reversible, and outward flow of protons through ATP synthase causes ATP hydrolysis. The PMF is the sum of two components, ΔpH and Δψ (the electric potential). These two components are equivalent for manipulating the direction of ATP synthase rotation, and thus its behavior as an ATP synthase or as an ATP hydrolase(Wiedenmann et al., 2008). If conditions that affect the direction or rate ATP synthase activity in turn affect T7 genome translocation, we will have evidence that there is a functional relationship between ATP synthase and the phage DNA delivery machinery. We have already observed a pH-dependent difference in lysis between T7 grown on WT *E. coli* and T7 growth on Δatp *E. coli*. While pH homeostasis is carefully regulated---*E. coli* maintains an internal pH between 7.6 and 7.8(Salmond et al., 1984; Slonczewski et al., 1981; Thomas et al., 2001), when cells are shifted from media at neutral pH to media at an acidic pH, protons

rapidly flux inward, driving the internal pH to 6.5 or lower within 20 seconds(Wilks & Slonczewski, 2007). The internal pH recovers to 7 over the next ten seconds, and then gradually returns to its baseline value over the course of five minutes(Wilks & Slonczewski, 2007). The The c-ring of ATP synthase conducts protons across the inner membrane of *E. coli*; upon a shift to an acidic environment, as protons flux inward to equilibrium, if ATP synthase is present, protons will flow through it, causing a rapid and transient increase in ATP synthesis.

To determine if the observed pH-dependent difference in lysis timing between a T7-infected WT or Δatp hosts is reflective of a change in the rate of DNA entry, we performed our entry experiments at pH 6, pH 7, and pH 8. We found that above and below neutral pH, the rate of DNA entry was slower on a Δatp host (**Fig. 3.5A**) To determine if the activity of ATP synthase affects T7 DNA translocation, we inhibited host transcription with rifampicin, and then shifted WT or Δatp *E. coli* from media at pH 7, to media at pH 6, infected with our panel of T7 variants, and performed our entry assays. As a control, we additionally treated cells, post-acid shift, with sodium acetate, a membrane permeable weak acid that can carry protons across the membrane, thus abolishing the PMF altogether. In the absence of transcription, WT T7, TI-T7, and ED-T7 cannot drive genome entry in WT or Δatp hosts (**Fig. 3.5B-D**). RED-T7, when ATP synthase is present, completes full genome entry within one minute after cells have been shifted to an acidic medium (**Fig. 3.5E**). When ATP synthase is absent, the genome of RED-T7 enters the cell at a constant rate, completing entry by 15 minutes post-infection. In the presence of acetate, the genome of RED-T7 does not enter the cell.

## DISCUSSION

The observation of an ordered complex of ATP synthase as part of the T7 DNA translocation apparatus suggests that T7 uses ATP synthase during the process of DNA ejection. The synthase complex is not visible in the earliest stage of adsorption, before the core proteins are ejected. The synthase complex appears coincidentally with the extended tail that safely conducts DNA from the phage capsid into the host cytoplasm. When the capsid is void of electron dense DNA, not only is the extended tail absent, but so, too, is the complex of ATP synthase. While ATP synthase is not required for T7 infection, its absence reduced the efficiency of plating by about half. Plaques on an ATP synthase deficient host also displayed a reduction in diameter and while plaques of T7 on a WT host will continue to increase in size on extended incubation, Δatp hosts failed to support this behavior. Lysis is delayed when T7 infects a host that lacks ATP synthase. The delay in lysis can be exacerbated by both a lowered pH as well as infection at a later stage of growth. At neutral pH, there is no obvious defect in DNA entry in the absence of ATP synthase: rates of overall entry, *Ec* RNAP-directed entry, and transcription-independent entry are the unaltered. However, when cells are grown at non-neutral pH, the rate of phage DNA entry is slower on a Δatp host. When cells are shifted into an acidic medium, the transient influx of protons into the cells coincides with the rapid egress of phage DNA into the host cytoplasm when ATP synthase is present and when the gp16 “brake” on DNA entry is absent.

The pH-dependent lysis delay of T7-infected Δatp hosts could reflect a physiological defect of such hosts at non-neutral pH. However, the pairing of this observation with the reduced rate of T7 DNA entry in Δatp hosts at non-neutral pH suggests that the delay specifically occurs at the point of entry and points to a role for the ΔpH component of the PMF in T7 DNA entry. *E. coli* maintains a near neutral internal pH.

When its environment is below neutral, transcription of several enzymes and transporters are altered to drive proton consumption and proton extrusion to maintain pH homeostasis (Slonczewski et al., 2009)—overall, the cell is working to move protons outward. When the environment is above neutral, *E. coli* upregulates ATP synthase to help drive protons inward and maintain a near neutral pH (Maurer et al., 2005). If T7 uses the PMF for transcription-independent entry, and recruits ATP synthase as an accessory factor for control of the PMF, then in the absence of ATP synthase, the effect of changed net proton flow on genome entry will be exaggerated.

Shifting cells from neutral media to acidic media induces a rapid, but transient influx of protons across the cell membrane. This can cause the rapid influx of T7 DNA, but only in the presence of ATP synthase, the absence of the T7 brake system, and the absence of RNAP promoters. That this requires the disengagement of the brake system makes sense: the gp16 DNA "clamp" is intrinsically engaged, and would otherwise prevent the genome from escaping the capsid. That this requires ATP synthase could also be reasoned out: the c-ring of ATP synthase is a proton channel, and a net movement of protons through it causes rapid ATP synthesis. T7 could be harnessing the locally increased ATP, or it could be engaging the proton flow through c-ring to drive rotation of its translocation channel to pull the genome at a faster rate. However, why the influx of DNA does not occur in a full-length T7 that has *Ec* RNAP promoters is unclear.

The transport of substrates across membranes often requires an energy source in the form of the proton motive force. Uncouplers of oxidative-phosphorylation like the protonophore CCCP, and ionophores like valinomycin have an inhibitory effect on bacterial secretion systems, the bacterial flagellum, and ATP synthase—all of which are rotary motors that use the flow of protons to drive rotation. The protonophore FCCP is known to arrest phage T7 transcription-independent DNA entry—the PMF is required for

transcription-independent DNA entry. There is an extensive network of homology between phage tails, bacterial secretion systems, and the bacterial flagellum (Abby & Rocha, 2012; Ginocchio et al., 1994; Nguyen et al., 2017; *Type VI Secretion System Translocates a Phage Tail Spike-like Protein into Target Cells Where It Cross-Links Actin | PNAS*, n.d.). The recruitment of ATP synthase to the phage T7 DNA translocon and its response to fluxes in the PMF analogous to the responses of the rotary motors of bacteria suggests that the T7 DNA too, may be a rotary motor. Future experiments should be done not only to better characterize the physical relationship between T7 and ATP synthase and the mechanism of DNA entry, but also to observe the specific mechanics of the machine they form together.

## MATERIALS AND METHODS

### Bacteria and Media:

Details on strains are listed in Table 1, and all are long-term residents of the laboratory collection. For lysis assays and one-step growth curves, the hosts were IJ2011, an *E. coli* BW25113 strain, and IJ2441, its *atp*-deficient derivative. Taehyun Park constructed IJ2441 by eliminating the ATP synthase operon of IJ2011 through P1 transduction of the ATP synthase deletion from strain DK8(Kaim & Dimroth, 1994). Deletion was verified through negative selection via growth on succinate—true knock outs are incapable of utilizing succinate as a carbon source(Boogerd et al., 1998; Butlin et al., 1971). For assays on DNA translocation, IJ1133 (WT) and IJ1525 (Δ*atp*) carrying the Dam-overexpressing plasmid, pTP166(Marinus et al., 1984) were the hosts.

Unless specified otherwise, cells were grown in a shaking water bath at 30˚C, in LB supplemented with 0.4% glucose, and buffered with 40 mM MOPS pH 7.0 to offset the acidification of the media observed when Δatp hosts ferment glucose.

### Phage:

Phages are listed in Table 2. For lysis and one step growth experiments, T7 was utilized and was grown on IJ2011. For experiments that required phages with completely unmethylated DNA, stocks were grown on *dam*-deficient hosts, either IJ922 or IJ1108 for phages that lacked gene 1. All phages were propagated and subsequently purified on a CsCl gradient, as historically described.(Studier, 1969) Phage titers were determined via plaque assay and stock was stored at 4˚C. To ensure repeatability of results, stock was only used for up to a month, after which time, synchronicity of infection is lost, though apparent titer remains unchanged. With the exception of one-step growth curves, all infections were at

an MOI of 5 and T7 buffer (10 mM tris-HCl, pH 8.0, 0.1 mM EDTA, 1 M NaCl) was utilized for dilution as necessary.

**Lysis and one-step growth assays:**

Cells were grown to a density of $2x10^8$ cells/mL in LB, 0.4% glucose, 40mM MOPS pH 7 in a shaking water bath at 30˚C. For acidic conditions, the buffer was 40 mM MES pH 6. For basic conditions, the buffer was 40mM Tricene pH 8. Phages were added to an MOI of 5 and the turbidity of the infected culture was followed through by measurement on a Klett-Summerson photoelectric colorimeter. Lysis of the culture was considered complete when the readings ceased to decrease and the media was clear.

For one step growth curves, cells were infected at an MOI of 0.1, and samples were extracted over time and treated with chloroform to artificially lyse the cells. Titers of released phage were enumerated on a plaque assay.

**DNA entry assay:**

This assay was performed largely according to the original design previously described by this lab(García & Molineux, 1995b). Cells containing the Dam-overexpressing plasmid pTP166 were grown in LB, 0.4% glucose, 40 mM MOPS pH 7 in a shaking water bath at 30˚C to a density of $2x10^8$ cells/mL. For experiments requiring the use of rifampin to inhibit host RNAP, the culture was centrifuged and the pellet resuspended in media containing 500 μg/mL of rifampin, pre-warmed to 30˚C and the culture was allowed to incubate for ten minutes before cells were infected. If chloramphenicol was required to shut off protein synthesis, then it was added to the culture

at a concentration of 200 μg/mL, and cells were incubated for 10 minutes prior to infection. Unmethylated phages, as appropriate to the experiment, were added at an MOI of 5.

For acid-shift experiments, when cells, grown in LB 0.4% glucose, 40 mM MOPS pH 7, reached a density of $2x10^8$ cells/mL, they were pelleted by centrifugation, resuspended in media containing 500 μg/mL rifampin, and 200 μg/mL chloramphenicol, and incubated at 30˚C, for ten minutes. Cells were then centrifuged and resuspended in LB 0.4% glucose, 40 mM MES pH 6.0 containing the mentioned concentrations of rifampin and chloramphenicol, and then immediately infected with unmethylated phage at an MOI of 5. After two minutes post-infection, the culture was split, and half the cells were treated with 40 mM potassium acetate.

To stop all cellular processes and harvest all DNA, we utilized the method outlined by Paetkau et al(Paetkau et al., 1975). At defined intervals post-infection, 750 μL of infected cells were added to an equal volume of ice-cold killing solution (75% EtOH; 2% phenol; 20 mM NaAcetate, pH 5.3; 8 mM EDTA pH 8.0; 15 mM NaOH), vortexed for 10 seconds, and placed on ice for the duration of the infection. Subsequently, samples were spun down at 13K RPM for 5 minutes to pellet DNA and other cellular debris. The supernatant was discarded, and the samples were either immediately processed, or stored at -20˚C to await processing.

Samples were then gently resuspended in 500 μL of TES (50 mM Tris-hydrochloride, pH 8.0; 25 mM EDTA; 50 mM NaCl) containing 0.5% SDS and 50 μg/mL Proteinase K. Proteinase K digestion was carried out at 55˚C for one hour, and 200 μL phenol equilibrated to pH 8 was added to remove protein and Proteinase K from the solution. RnaseA was added at 0.2 mg/mL and RNA was digested for one hour at 37˚C. Two rounds of phenol/chloroform/isoamyl alcohol treatment followed for clean-up, and DNA was ethanol precipitated and resuspended in 50 μL di$H_2O$.

25 μL of DNA from each time point was digested with enzymes from New England Biolabs (NEB), according to NEB protocols. For the first time point, Sau3AI was used to digest all DNA within the sample, and all other time points were digested with Dpn I to selectively cleave methylated DNA. Digests were run on a 1% agarose gel at 20V for 10 hours. Gels were stained with 1:1000 dilutions of SYBR Gold in TBE buffer, prepared according to Cold Spring Harbor protocols("TBE Buffer," 2006), for 30 minutes, and DNA was imaged on the Typhoon 9500. Images were labeled and quantified using ImageJ(Schneider et al., 2012) and GelAnalyzer 19.1(Lazar, Jr & Lazar, Sr, n.d.).

**Analysis of DNA:**

For plotting the amount of DNA entered into a cell at a given time, the appearance of phage-specific bands on an agarose gel were used to estimate the amount of DNA in a cell. All experiments were done in triplicate and data was analyzed and visualized with R(R Core Team, 2021), run on RStudio(RStudio Team, 2022) with the packages dplyr, ggforce, ggplot2, scales, and tidyr. Figures were created using BioRender (BioRender.com).

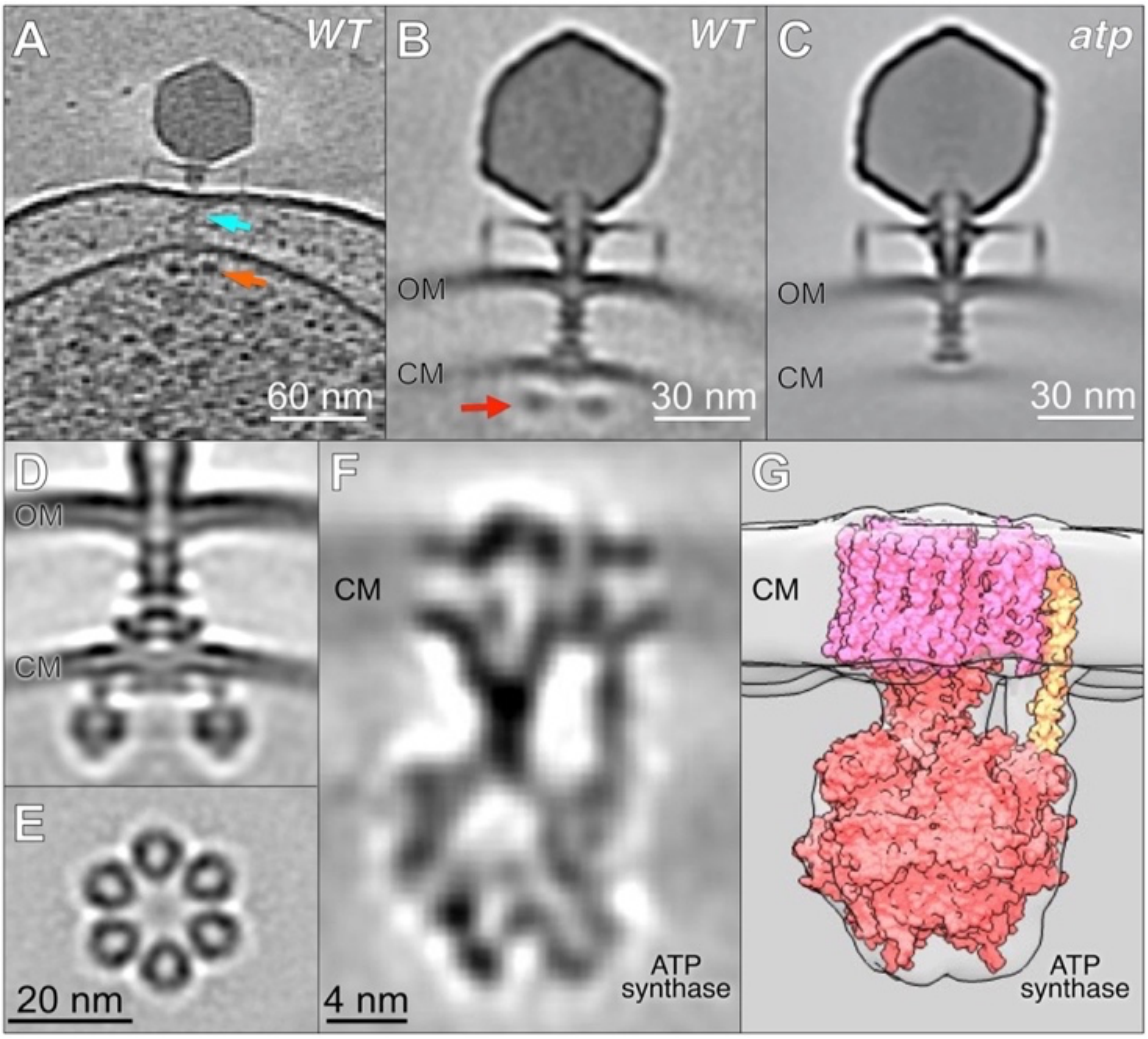


**Figure 3.1**. Bacteriophage T7 recruits ATP synthase at the initiation of infection

**(A)** 3D reconstructions reveal a sub-class of adsorbed T7 that exhibits an extended tail across the cellular envelope (blue arrow) and an area of electron density (red arrow) at the cytoplasmic face of the cell membrane (CM). **(B)** Further selection and refinement shows a higher resolution structure (red arrow). **(C)** The structure is absent when T7 infects a Δatp

host. **(D)** A central slice shows ordered arrangement at the base of phage T7's DNA translocation apparatus. **(E)** End on view reveals a hexamer surrounding a central pore. **(F)** Slice of an averaged subunit of the hexamer shows the full ATP synthase. **(G)** The atomic structure of ATP synthase docked to the CryoET density.

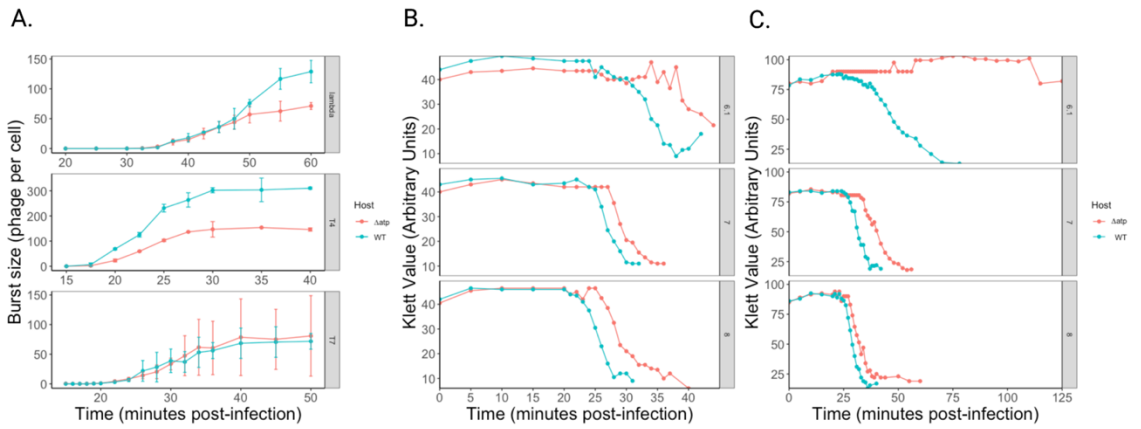


**Fig. 3.2**. Absence of ATP synthase causes a conditional defect for phage T7

**(A)** One-step growth curves of lambda-*vir*, T4, and T7 on a WT or Δatp *E. coli* host. Cells were grown to mid-log in LB, 0.4% glucose, 40 mM MOPS pH 7 at 37˚C for lambda and T4 infections, and 30˚C for T7 infections. Cells were infected at an MOI of 0.1, and cells were artificially lysed at the given time points and plated to determine the number of phages in a cell over time. Data shown are the average of three biological replicates, with error bars showing plus or minus standard deviation. A reduction in burst size is observed when lambda-*vir* or T4 infects a Δatp host. T7 exhibited highly variable behavior on a Δatp host. **(B & C)** Lysis curves—cells were grown in LB, 0.4% glucose buffered with either 40 mM MOPs pH7, 40 mM MES pH 6.1, or 40 mM Tricene pH 8.0 and infected with T7 at an MOI of 5. **(B)**WT or Δatp hosts were infected with T7 at pH 6.1, pH 7, or pH 8 at mid-log and a delay in lysis is observed that varies with pH. **(C)** WT or Δatp hosts grown at pH 6.1, pH 7, or pH 8 were infected at late mid-log, and the delay in lysis was extended at the lower values.

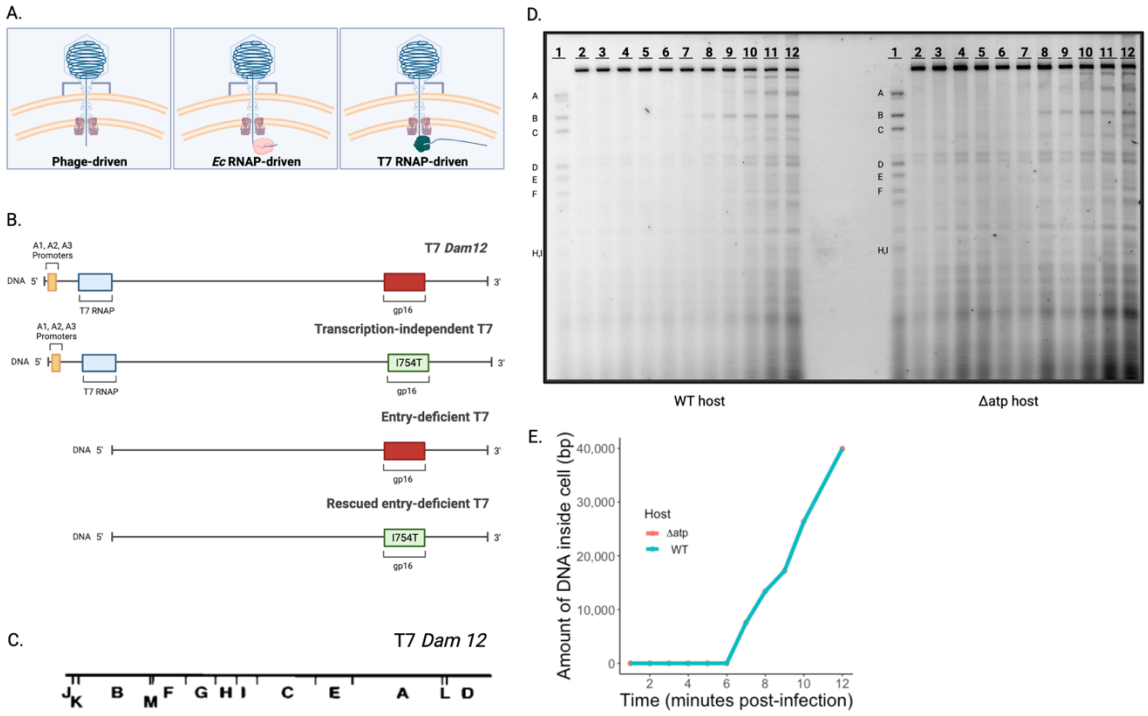


**Figure 3.3**. DNA entry experiments show no obvious role for ATP synthase during bulk T7 genome translocation

**(A)** A graphic representation of the phage T7's tripartite mechanism of DNA delivery; the first 1kb enter through a phage-driven process; the next 7 kb are pulled into the cell by host transcription; the remainder of the genome enters by T7 RNAP transcription. **(B)** A representation of the genomes of the T7 variants used for the entry experiment showing relevant DNA entry control elements. **(C)** Linear map of DpnI cut sites along T7 Dam12 genome, with each fragment formed lettered from A-M based on size in bp. **D)** SYBR Gold stained agarose gel of restriction digest treated phage DNA. IJ1133 (WT) or IJ1525 (Δatp) cells overexpressing *dam* were grown to mid-log at 30˚C in LB, 4% glucose, 40 mM MOPS, pH 7, and infected with phage at an MOI of 5. As phage DNA enters a cell, it

becomes methylated. At various time points, DNA was extracted, digested with Dpn I, which only cuts methylated DNA, and run on a 1% gel. Bands are formed when Dpn I cleaves at vulnerable loci along the genome. Their appearance on a gel coincides with time of entry of that vulnerable locus into a cell. Numbers across top of lanes represents minutes post-infection. Resolvable fragments are labeled with letters from A-I for the control lanes for each condition and correspond to the regions labeled in C. **(E)** Amount of T7 Dam12 DNA inside a host cell over time. Plot of approximate length of DNA within a cell over time based on D. ATP synthase absence does not affect the overall process of phage T7 DNA entry.

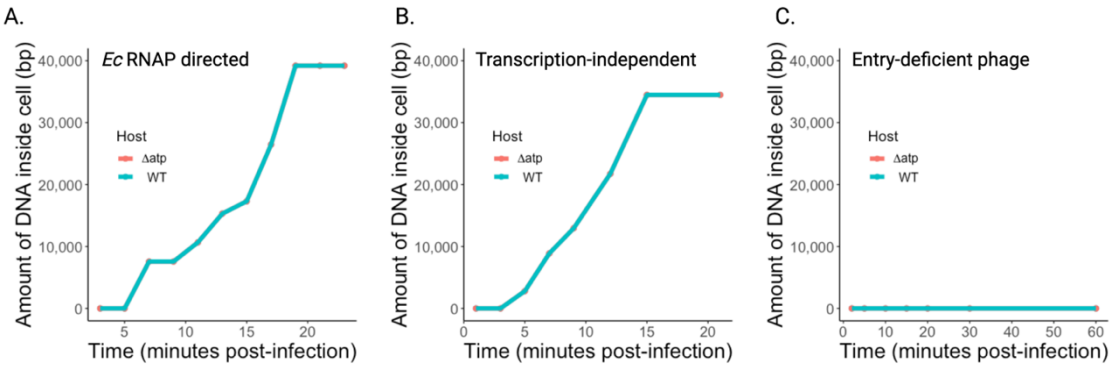


**Figure 3.4**. DNA entry experiments show no obvious role for ATP synthase during T7 genome translocation

**A-C)** Plots of length of phage DNA entered into a cell over time. DNA entry was performed: IJ1133 (WT) or IJ1525 (Δatp) cells overexpressing *dam* were grown to mid-log at 30˚C in LB, 4% glucose, 40 mM MOPS, pH 7, and infected with phage at an MOI of 5. As phage DNA enters a cell, it becomes methylated. At various time points, DNA was extracted, digested with Dpn I, which only cuts methylated DNA, and run on a 1% gel. Bands are formed when Dpn I cleaves at vulnerable loci along the genome. Their appearance on a gel coincides with time of entry of that vulnerable locus into a cell. This was used to approximate amount of DNA within a cell and was plotted over time. **A)** Plot of *Ec.* RNAP directed T7 DNA entry. DNA entry experiment as described, but cells were treated with 200 μg/mL chloramphenicol ten minutes prior to infection with T7 Dam12 to prevent translation of phage proteins, particularly gene 1. Absence of ATP synthase did not affect entry, and plots of entered DNA on WT or Δatp host overlap. **B)** Plot of T7 transcription-independent DNA entry. DNA entry assay as described, but ten minutes prior to infection, cells were treated with 500 μg/mL rifampin to inhibit *Ec.* RNAP and 200 μg/mL chloramphenicol to prevent translation. Cells were then infected with phages with a transcription-independent mechanism of DNA entry (T7 Dam12, *16I754T*). Absence of

ATP synthase did not affect the rate of transcription independent DNA entry, and plots on hosts overlap. **C)** Plot of DNA entry over time of a phage lacking *E. coli* RNAP promoters and T7 gene 1. DNA entry assay was performed as described on cells infected with Entry-deficient T7 phages (T7 *D394-5911*, Dam10). The absence of ATP synthase did not allow these phages to eject their genomes into a host.

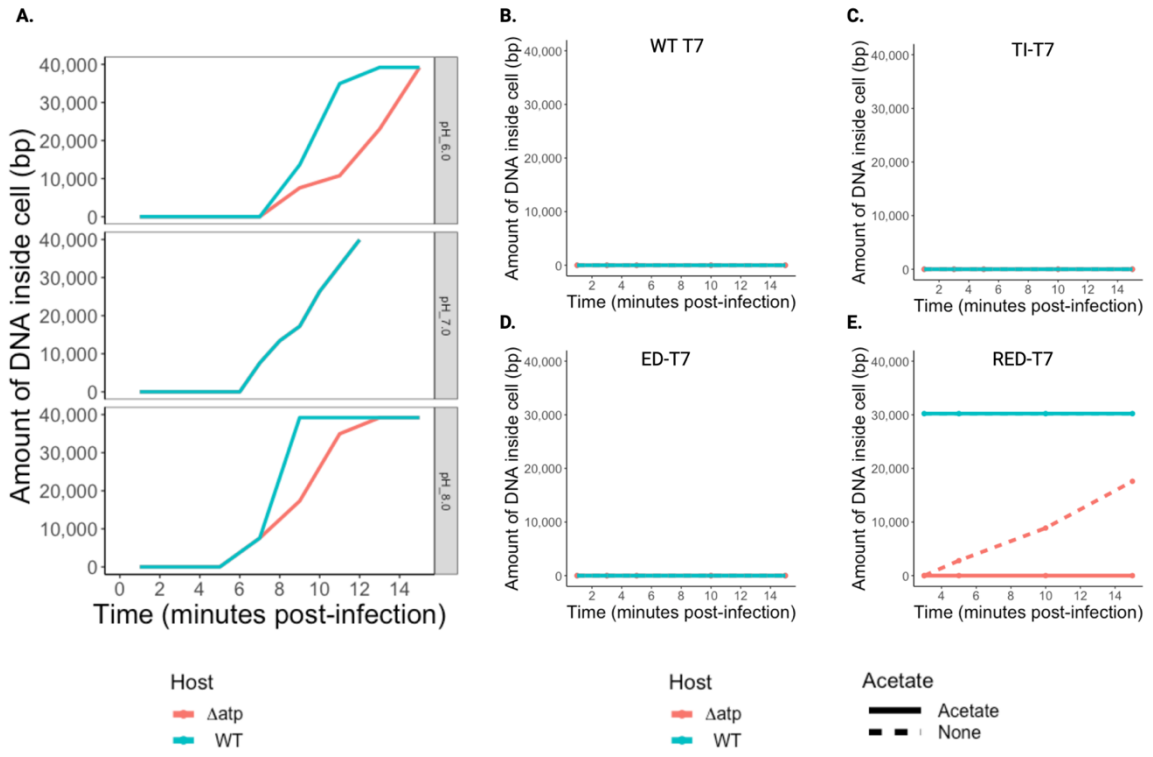


**Figure 3.5**. Rate of phage T7 DNA entry is slower in a Δatp host when the pH is above or below neutral. In the absence of transcription, disengagement of the T7 gp16 "brake" allows proton flow through ATP synthase to drive rapid phage DNA entry

**A-E)** Plots of the apparent length of phage DNA inside a host cell over time. **A)** Cells overexpressing *dam* were grown to mid-log at 30˚C in LB buffered to pH 6, 7, or 8 and infected with T7 Dam12 at an MOI of 5. As phage DNA enters a cell, it becomes methylated. At various time points, DNA was extracted, digested with Dpn I, which only cuts methylated DNA, and run on a gel. Bands are formed when Dpn I cleaves at vulnerable loci along the genome. Their appearance on a gel coincides with time of entry of that vulnerable locus into a cell, and is used to plot approximate length of DNA within a cell over time. At pH 6, the rate of entry of T7 DNA was slower in a Δatp host. At pH 7, there

was no difference in the rate of DNA entry between a WT and Δatp host. At pH 8, the rate of genome entry was slower in a Δatp host. **(B-E)** Plots of DNA Entry assay as in A, but cells were grown at pH 7, treated with 500 ug/mL rifampicin for 10 minutes prior to infection, then spun down and resuspended in rifampicin containing media at pH 6.0 and then immediately infected with phage at an MOI of 5. At two-minutes post-infection, the culture was split and one half was treated with 40 mM KAcetate, which abolishes the proton-motive force. **(B)** Dam 12 phage DNA does not enter the cell in these conditions. **(C)** Phages with a transcription-independent mechanism of DNA entry (T7 Dam12, *16I754T*) cannot eject their DNA into cells in these conditions. **(D)** Entry-deficient T7 phages (T7 *D394-5911*, Dam10) do not eject their DNA after a shift to acidic media. (**E)** Rescued entry-deficient T7 phages, (T7 *D394-5911*, Dam10, *16I754)* eject their DNA after a shift into acidic media.

Table 3.1. E. coli strains used in this work

| Strain | Genotype | Source |
|---|---|---|
| **IJ511*dam-13::Tn9*** | Δ*lacX74*, *galK2, galT22, supE44, hsdS, dam-13::Tn9* | Garcia and Molineux, 1995 |
| **IJ922** | K-12 *lacX74, supE44, galK2, galT22, mcrA, rfbD1, dam-13::Tn9, mcrB1, hsdS3* | Struthers-Schlinke, Molineux, 2000 |
| **IJ1133** | Δ*lacX74*, Δ(*mcrC-mrr*)102::Tn10 | Garcia and Molineux, 1995 |
| **IJ1134** | Δ*lacX74*, Δ(*mcrC-mrr*)102::Tn10, *lacUV5, lacZ::T7 gene1-Kn*$^{R}$ | Garcia and Molineux, 1995 |
| **IJ1525** | Δ*lacX74*, Δ*thi*, Δ(*mcrC-mrr*)102::Tn10Δ*(uncB-uncC) ilv::Tn10* | Kemp, Molineux, 2004 |
| **IJ2011** | *Δ(araD-araB)567, ΔlacZ4787(::rrnB-3), λ*$^{-}$*, rph-1, Δ(rhaD-rhaB)568, hsdR514* | Molineux Laboratory catalogue |
| **IJ2441** | *Δ(araD-araB)567, ΔlacZ4787(::rrnB-3), λ*$^{-}$*, rph-1, Δ(rhaD-rhaB)568, hsdR514,* Δ*(atpB-atpC)ilv::Tn10* | Taehyun Park, for the Molineux Laboratory catalogue |

Table 3.2. Phages used in this work

| Bacteriophage | Description | Source |
|---|---|---|
| **T7$^+$** | Deposited in the ATCC as BAA-1025-B2 | William Studier |
| **T7 Dam12** | Has 6 additional Dpn I cut sites (GATC sequences) added variously through ligation of the WT phage with cloning sites and T7 variants known to harbor extra GATC sites. Functionally wild-type. | Garcia and Molineux, 1995 |
| **T7 Dam12, *16I754T*** | The product of ligation of T7 Dam 12 with the right hand portion of a phage from the Studier collection. Bears a point mutation in gp16 resulting in an I to T change at residue 754. This is sufficient to allow the phage to complete genome entry into a host in the absence of transcription. | Garcia and Molineux, 1996 |
| **T7 D394-5911, Dam10** | Product of the recombination of T7 4101 from the Studier lab with T7 bearing extra GATC sites. The deletion it bears removes the A1, A2, A3, B, and C promoters as well as genes 0.3-1. It cannot facilitate genome entry unless the host ectopically expresses T7 gene 1 | Struthers-Schlinke, Molineux, 2000 |
| **T7 D394-5911, Dam10, *16I754T*** | Same as T7 D394-5911, Dam 10, but bearing the gp16 I754T mutation rendering it able to complete genome entry in the absence of transcription | |
| **λcI** | Phage lambda with a mutation in the repressor protein, preventing lysogeny and rendering this phage obligately lytic | Molineux Laboratory collection |
| **T4rI** | Bacteriophage T4 | Molineux Laboratory collection |

# CHAPTER 4: DISCUSSION

Bacteriophage T7 is, essentially, a parasite of bacteria reduced to one fundamental purpose: to spread its genome. Tracing the process of genetic invasion and amplification with a reliable bulk assay has historically involved the use of radiolabeled nucleotides---costly, with a short shelf life, and, in the case of T7 DNA replication, perhaps not a reliable reporter. In this dissertation, in **Chapter 2**, I describe how I've modified the DNA translocation assay pioneered in this lab for use as a readout for DNA replication and evaluated its utility as a tool for DNA replication study. In **Chapter 3**, I investigate how ATP synthase, coincidentally observed at the formation of the T7 DNA translocation apparatus, might be utilized in the process of DNA entry, using a modification of this lab's DNA entry assay as a primary means of investigation. By this method, there was no obvious role for ATP synthase during DNA entry, and a defect in entry in the absence of ATP synthase was only observed when cells were either adapted to non-neutral pH conditions, or when cells were shifted to from a neutral pH to an acidic pH. In the latter case, the defect was only apparent for cells that lacked promoters for host RNA polymerase and had a mutation in gp16---a core protein ejected to form part of the DNA translocation apparatus that prevents ejection of phage DNA past the first 1,000 bp in the absence of transcription. The mutant gp16 used in this experiment allows for transcription-independent DNA entry. These results, at a glance, are hard to reconcile. However, they provide a promising platform from which to launch future investigations.

The results in **Chapter 3** suggest that T7 nucleic acid transport is driven in part by the membrane potential. To better characterize the role of the proton motive force in T7 DNA translocation and to tie it to ATP synthase, one might revisit the pioneering experiments utilized to characterize the nature of ATP synthase (Maloney et al., 1974) and the function of the bacterial flagellum (Manson et al., 1977). For each molecular machine, experiments manipulated the electric potential and the pH gradient to find a corresponding effect in the rate of ATP synthesis, and the motility of bacteria, respectively. For characterizing T7 DNA translocation, the readout would necessarily be

rate of genome entry into a host cell. Mid-log phase *E. coli* maintain an intracellular $K^+$ concentration of ~200 mM (Schultz & Solomon, 1961), while LB has a $K^+$ concentration of ~ 7 mM (Kuo et al., 2003). An inward-directed proton motive force can be generated by the addition of valinomycin, which makes the cell permeable to potassium, initiating an efflux of potassium that results in a net negative electric potential (Glynn, 1967). In response to such a shift, cells compensate with an influx of protons for ~two minutes—ATP synthesis consequently increases; if T7 couples proton flow with genome translocation, then DNA translocation would rapidly occur. In the absence of ATP synthase, cells do not exhibit an increase in ATP synthesis after valinomycin treatment. If in the absence of ATP synthase T7 DNA translocation increases in rate after valinomycin treatment to the same degree observed in a WT cell, then the relationship between T7 and ATP synthase observed in this dissertation falls apart. However, if valinomycin treatment triggers rapid T7 genome egress only in the presence of ATP synthase, then a relationship between T7 and this molecular machine becomes more certain.

If the link between T7 genome translocation and ATP synthase can be proven more robustly, there is much food and fruit here for future years. Defining the molecular interaction between ATP synthase and the T7 DNA translocation apparatus is obvious low-hanging fruit. A pull-down experiment paired with mass-spectroscopy would allow us to identify the interacting residues between ATP synthase and T7's core proteins. Defining the points of interaction would enable construction of a more detailed structural model. On the assumption that the translocation apparatus is a molecular motor, one might ask if the T7 complex rotates. A possible readout would be a microscopy experiment—bacteria could be added to a flow cell treated with poly-L-lysine to immobilize cells. Phage T7 with a strep-tag to the c-terminus of gp10, the phage capsid protein, could be added, followed by strep-avidin beads. Observation of the capsid-bound bead over time would allow read out of motion of the phage complex. Phylogenetic studies would allow relationships to be drawn between phage DNA ejection complexes and provide a rationale to launch experiments to determine if recruitment of ATP synthase is a common mechanism for tailed phages.

Overall, while the work presented here is brief, it is nevertheless a useful launchpad for thought. It showcases how tailed bacteriophages, while simple in nature and well-studied, harbor yet more biological curiosities. Further, it provides groundwork for future studies—there's rich material for years more of investigation into the early life cycle of phage T7.

# References


Abby, S. S., & Rocha, E. P. C. (2012). The Non-Flagellar Type III Secretion System Evolved from the Bacterial Flagellum and Diversified into Host-Cell Adapted Systems. *PLOS Genetics*, *8*(9), e1002983. https://doi.org/10.1371/journal.pgen.1002983

Adams, Mark Hancock. (1959). *Bacteriophages*. Interscience Publishers. http://www.archaealviruses.org/citations/adams_1959.html

Benzer, S. (1959). On the topology of the genetic fine structure. *Proceedings of the National Academy of Sciences*, *45*(11), 1607–1620. https://doi.org/10.1073/pnas.45.11.1607

Bernheim, A., Millman, A., Ofir, G., Meitav, G., Avraham, C., Shomar, H., Rosenberg, M. M., Tal, N., Melamed, S., Amitai, G., & Sorek, R. (2021). Prokaryotic viperins produce diverse antiviral molecules. *Nature*, *589*(7840), Article 7840. https://doi.org/10.1038/s41586-020-2762-2

Bobonis, J., Mitosch, K., Mateus, A., Karcher, N., Kritikos, G., Selkrig, J., Zietek, M., Monzon, V., Pfalz, B., Garcia-Santamarina, S., Galardini, M., Sueki, A., Kobayashi, C., Stein, F., Bateman, A., Zeller, G., Savitski, M. M., Elfenbein, J. R., Andrews-Polymenis, H. L., & Typas, A. (2022). Bacterial retrons encode phage-defending tripartite toxin-antitoxin systems. *Nature*, *609*(7925), 144–150. https://doi.org/10.1038/s41586-022-05091-4

Boogerd, F. C., Boe, L., Michelsen, O., & Jensen, P. R. (1998). Atp Mutants of Escherichia coli Fail To Grow on Succinate Due to a Transport Deficiency. *Journal of Bacteriology*, *180*(22), 5855–5859.

Burnet, F. M. (1927). The Relationships between Heat-Stable Agglutinogens and Sensitivity to Bacteriophage in the Salmonella Group. *British Journal of Experimental Pathology*, *8*(2), 121–129.

Burnet, F., & McKie, M. (1929). OBSERVATIONS ON A PERMANENTLY LYSOGENIC STRAIN OF *B. ENTERITIDIS GAERTNER*. *Australian Journal of Experimental Biology and Medical Science*, *6*(4), 277–284. https://doi.org/10.1038/icb.1929.26

Burstein, D., Harrington, L. B., Strutt, S. C., Probst, A. J., Anantharaman, K., Thomas, B. C., Doudna, J. A., & Banfield, J. F. (2017). New CRISPR–Cas systems from

uncultivated microbes. *Nature*, *542*(7640), Article 7640. https://doi.org/10.1038/nature21059

Butlin, J. D., Cox, G. B., & Gibson, F. (1971). Oxidative phosphorylation in Escherichia coli K12. Mutations affecting magnesium ion- or calcium ion-stimulated adenosine triphosphatase. *The Biochemical Journal*, *124*(1), 75–81. https://doi.org/10.1042/bj1240075

Calendar, R. (Ed.). (2006). *The bacteriophages* (2nd ed). Oxford University Press.

Callanan, J., Stockdale, S. R., Shkoporov, A., Draper, L. A., Ross, R. P., & Hill, C. (2020). Expansion of known ssRNA phage genomes: From tens to over a thousand. *Science Advances*, *6*(6), eaay5981. https://doi.org/10.1126/sciadv.aay5981

Center, M. S. (1973). Bacteriophage T7 DNA Synthesis in Isolated DNA-Membrane Complexes. *Journal of Virology*, *12*(4), 847–854. https://doi.org/10.1128/jvi.12.4.847-854.1973

Cerritelli, M. E., Cheng, N., Rosenberg, A. H., McPherson, C. E., Booy, F. P., & Steven, A. C. (1997). Encapsidated conformation of bacteriophage T7 DNA. *Cell*, *91*(2), 271–280. https://doi.org/10.1016/s0092-8674(00)80409-2

Chaikeeratisak, V., Khanna, K., Nguyen, K. T., Egan, M. E., Enustun, E., Armbruster, E., Lee, J., Pogliano, K., Villa, E., & Pogliano, J. (2022). Subcellular organization of viral particles during maturation of nucleus-forming jumbo phage. *Science Advances*, *8*(18), eabj9670. https://doi.org/10.1126/sciadv.abj9670

Chaikeeratisak, V., Nguyen, K., Khanna, K., Brilot, A. F., Erb, M. L., Coker, J. K. C., Vavilina, A., Newton, G. L., Buschauer, R., Pogliano, K., Villa, E., Agard, D. A., & Pogliano, J. (2017). Assembly of a nucleus-like structure during viral replication in bacteria. *Science*, *355*(6321), 194–197. https://doi.org/10.1126/science.aal2130

Chang, C.-Y., Kemp, P., & Molineux, I. J. (2010). Gp15 and gp16 cooperate in translocating bacteriophage T7 DNA into the infected cell. *Virology*, *398*(2), 176–186. https://doi.org/10.1016/j.virol.2009.12.002

Chung, Y.-B., & Hinkle, D. C. (1990a). Bacteriophage T7 DNA Packaging: I. Plasmids containing a T7 replication origin and the T7 concatemer junction are packaged into transducing particles during phage infection. *Journal of Molecular Biology*, *216*(4), 911–926. https://doi.org/10.1016/S0022-2836(99)80010-2

Chung, Y.-B., & Hinkle, D. C. (1990b). Bacteriophage T7 DNA Packaging: II. Analysis of the DNA sequences required for packaging using a plasmid transduction assay. *Journal of Molecular Biology*, *216*(4), 927–938. https://doi.org/10.1016/S0022-2836(99)80011-4

Cohen, D., Melamed, S., Millman, A., Shulman, G., Oppenheimer-Shaanan, Y., Kacen, A., Doron, S., Amitai, G., & Sorek, R. (2019). Cyclic GMP–AMP signalling protects bacteria against viral infection. *Nature*, *574*(7780), Article 7780. https://doi.org/10.1038/s41586-019-1605-5

Condon, C., French, S., Squires, C., & Squires, C. L. (1993). Depletion of functional ribosomal RNA operons in Escherichia coli causes increased expression of the remaining intact copies. *The EMBO Journal*, *12*(11), 4305–4315.

Cong, L., Ran, F. A., Cox, D., Lin, S., Barretto, R., Habib, N., Hsu, P. D., Wu, X., Jiang, W., Marraffini, L. A., & Zhang, F. (2013). Multiplex genome engineering using CRISPR/Cas systems. *Science (New York, N.Y.)*, *339*(6121), 819–823. https://doi.org/10.1126/science.1231143

Crick, F. H. C., Barnett, L., Brenner, S., & Watts-Tobin, R. J. (1961). General Nature of the Genetic Code for Proteins. *Nature*, *192*(4809), Article 4809. https://doi.org/10.1038/1921227a0

Daugelavicius, R., Bamford, J. K., & Bamford, D. H. (1997). Changes in host cell energetics in response to bacteriophage PRD1 DNA entry. *Journal of Bacteriology*, *179*(16), 5203–5210.

Delbruck, M. (1978, September 14). *Interview with Max Delbruck by Carolyn Harding* [Interview]. https://resolver.caltech.edu/CaltechOH:OH_Delbruck_M

Delbrück, M., & Bailey, W. T. (1946). Induced Mutations in Bacterial Viruses. *Cold Spring Harbor Symposia on Quantitative Biology*, *11*, 33–37. https://doi.org/10.1101/SQB.1946.011.01.006

Demerec, M., & Fano, U. (1945). Bacteriophage-Resistant Mutants in Escherichia Coli. *Genetics*, *30*(2), 119–136.

Deng, X., Wang, L., You, X., Dai, P., & Zeng, Y. (2018). Advances in the T7 phage display system (Review). *Molecular Medicine Reports*, *17*(1), 714–720. https://doi.org/10.3892/mmr.2017.7994

D'Herelle, F. (1911). Sur une epizootie de nature bacterienne sevissant sur les sauterelles au Mexique. *Comptes Rendus Hebdomadaires Des Séances de l'Académie Des Sciences*, *152*, 1413–1415.

D'Herelle, F. (1917). Sur un microbe invisible antagoniste des bacilles dysenteriques. *Comptes Rendus Hebdomadaires Des Séances de l'Académie Des Sciences*, *165*, 373–375.

D'Herelle, F. (1926). *The bacteriophage and its behavior*. The Williams & Wilkins company.

Doron, S., Melamed, S., Ofir, G., Leavitt, A., Lopatina, A., Keren, M., Amitai, G., & Sorek, R. (2018). Systematic discovery of antiphage defense systems in the microbial pangenome. *Science*, *359*(6379), eaar4120. https://doi.org/10.1126/science.aar4120

Dressler, D., Wolfson, J., & Magazin, M. (1972). Initiation and reinitiation of DNA synthesis during replication of bacteriophage T7. *Proceedings of the National Academy of Sciences of the United States of America*, *69*(4), 998–1002. https://doi.org/10.1073/pnas.69.4.998

Dunn, J. J., & Studier, F. W. (1980). The transcription termination site at the end of the early region of bacteriophage T7 DNA. *Nucleic Acids Research*, *8*(10), 2119–2132.

Dunn, J. J., Studier, F. W., & Gottesman, M. (1983). Complete nucleotide sequence of bacteriophage T7 DNA and the locations of T7 genetic elements. *Journal of Molecular Biology*, *166*(4), 477–535. https://doi.org/10.1016/S0022-2836(83)80282-4

Edgar, B. (2004). The Genome of Bacteriophage T4. *Genetics*, *168*(2), 575–582.

Egelman, E. H., Yu, X., Wild, R., Hingorani, M. M., & Patel, S. S. (1995). Bacteriophage T7 helicase/primase proteins form rings around single-stranded DNA that suggest a general structure for hexameric helicases. *Proceedings of the National Academy of Sciences of the United States of America*, *92*(9), 3869–3873. https://doi.org/10.1073/pnas.92.9.3869

Ellis, E. L., & Delbrück, M. (1939). THE GROWTH OF BACTERIOPHAGE. *The Journal of General Physiology*, *22*(3), 365–384.

Epstein, R. H., Bolle, A., & Steinberg, C. M. (2012). Amber Mutants of Bacteriophage T4D: Their Isolation and Genetic Characterization1. *Genetics*, *190*(3), 831–840. https://doi.org/10.1534/genetics.112.138438

Fuller, C. W., & Richardson, C. C. (1985). Initiation of DNA replication at the primary origin of bacteriophage T7 by purified proteins. Site and direction of initial DNA synthesis. *The Journal of Biological Chemistry*, *260*(5), 3185–3196.

García, L. R., & Molineux, I. J. (1995a). Incomplete entry of bacteriophage T7 DNA into F plasmid-containing Escherichia coli. *Journal of Bacteriology*, *177*(14), 4077–4083.

García, L. R., & Molineux, I. J. (1995b). Rate of translocation of bacteriophage T7 DNA across the membranes of Escherichia coli. *Journal of Bacteriology*, *177*(14), 4066–4076. https://doi.org/10.1128/jb.177.14.4066-4076.1995

García, L. R., & Molineux, I. J. (1996). Transcription-independent DNA translocation of bacteriophage T7 DNA into Escherichia coli. *Journal of Bacteriology*, *178*(23), 6921–6929. https://doi.org/10.1128/jb.178.23.6921-6929.1996

García, L. R., & Molineux, I. J. (1999). Translocation and specific cleavage of bacteriophage T7 DNA in vivo by EcoKI. *Proceedings of the National Academy of Sciences*, *96*(22), 12430–12435. https://doi.org/10.1073/pnas.96.22.12430

Gasiunas, G., Barrangou, R., Horvath, P., & Siksnys, V. (2012). Cas9-crRNA ribonucleoprotein complex mediates specific DNA cleavage for adaptive immunity in bacteria. *Proceedings of the National Academy of Sciences of the United States of America*, *109*(39), E2579-2586. https://doi.org/10.1073/pnas.1208507109

Ginocchio, C. C., Olmsted, S. B., Wells, C. L., & Galán, J. E. (1994). Contact with epithelial cells induces the formation of surface appendages on Salmonella typhimurium. *Cell*, *76*(4), 717–724. https://doi.org/10.1016/0092-8674(94)90510-X

Glynn, I. M. (1967). Involvement of a Membrane Potential in the Synthesis of ATP by Mitochondria. *Nature*, *216*(5122), Article 5122. https://doi.org/10.1038/2161318a0

Hayes, William. (1982). Max Ludwig Henning Delbrück, 4 September 1906—10 March 1981. *Biographical Memoirs of Fellows of the Royal Society*, *28*, 59–90. https://doi.org/10.1098/rsbm.1982.0003

Hershey, A. D. (1946a). Mutation of Bacteriophage with Respect to Type of Plaque. *Genetics*, *31*(6), 620–640.

Hershey, A. D. (1946b). Spontaneous Mutations in Bacterial Viruses. *Cold Spring Harbor Symposia on Quantitative Biology*, *11*, 67–77. https://doi.org/10.1101/SQB.1946.011.01.010

Hershey, A. D., Burgi, E., & Ingraham, L. (1963). COHESION OF DNA MOLECULES ISOLATED FROM PHAGE LAMBDA. *Proceedings of the National Academy of Sciences of the United States of America*, *49*(5), 748–755.

Hershey, A. D., & Chase, M. (1952). Independent functions of viral protein and nucleic acid in growth of bacteriophage. *The Journal of General Physiology*, *36*(1), 39–56.

Hershey, A. D., & Rotman, R. (1948). Linkage Among Genes Controlling Inhibition of Lysis in a Bacterial Virus. *Proceedings of the National Academy of Sciences of the United States of America*, *34*(3), 89–96.

Hinkle, D. C. (1980). Evidence for direct involvement of T7 RNA polymerase bacteriophage DNA replication. *Journal of Virology*, *34*(1), 136–141. https://doi.org/10.1128/jvi.34.1.136-141.1980

Hori, K., Mark, D. F., & Richardson, C. C. (1979). Deoxyribonucleic acid polymerase of bacteriophage T7. Characterization of the exonuclease activities of the gene 5 protein and the reconstituted polymerase. *Journal of Biological Chemistry*, *254*(22), 11598–11604. https://doi.org/10.1016/S0021-9258(19)86527-4

Hu, B., Margolin, W., Molineux, I. J., & Liu, J. (2013). The Bacteriophage T7 Virion Undergoes Extensive Structural Remodeling During Infection. *Science (New York, N.Y.)*, *339*(6119). https://doi.org/10.1126/science.1231887

Jagendorf, A. T., & Uribe, E. (1966). ATP formation caused by acid-base transition of spinach chloroplasts. *Proceedings of the National Academy of Sciences of the United States of America*, *55*(1), 170–177.

Jakutytė, L., Lurz, R., Baptista, C., Carballido-Lopez, R., São-José, C., Tavares, P., & Daugelavičius, R. (2012). First steps of bacteriophage SPP1 entry into Bacillus subtilis. *Virology*, *422*(2), 425–434. https://doi.org/10.1016/j.virol.2011.11.010

Jinek, M., Chylinski, K., Fonfara, I., Hauer, M., Doudna, J. A., & Charpentier, E. (2012). A programmable dual RNA-guided DNA endonuclease in adaptive bacterial immunity. *Science (New York, N.Y.)*, *337*(6096), 816–821. https://doi.org/10.1126/science.1225829

Johnson, A. G., Wein, T., Mayer, M. L., Duncan-Lowey, B., Yirmiya, E., Oppenheimer-Shaanan, Y., Amitai, G., Sorek, R., & Kranzusch, P. J. (2022). Bacterial gasdermins reveal an ancient mechanism of cell death. *Science*, *375*(6577), 221–225. https://doi.org/10.1126/science.abj8432

Kagawa, Y., & Racker, E. (1971). Partial Resolution of the Enzymes Catalyzing Oxidative Phosphorylation. *Journal of Biological Chemistry*, *246*(17), 5477–5487. https://doi.org/10.1016/S0021-9258(18)61930-1

Kaim, G., & Dimroth, P. (1994). Construction, expression and characterization of a plasmid-encoded Na+-specific ATPase hybrid consisting of Propionigenium modestum F0-ATPase and Escherichia coli F1-ATPase. *European Journal of Biochemistry*, *222*(2), 615–623. https://doi.org/10.1111/j.1432-1033.1994.tb18904.x

Kelly, T. J., & Smith, H. O. (1970). A restriction enzyme from Hemophilus influenzae. II. *Journal of Molecular Biology*, *51*(2), 393–409. https://doi.org/10.1016/0022-2836(70)90150-6

Kemp, P., Garcia, L. R., & Molineux, I. J. (2005). Changes in bacteriophage T7 virion structure at the initiation of infection. *Virology*, *340*(2), 307–317. https://doi.org/10.1016/j.virol.2005.06.039

Kemp, P., Gupta, M., & Molineux, I. J. (2004). Bacteriophage T7 DNA ejection into cells is initiated by an enzyme-like mechanism. *Molecular Microbiology*, *53*(4), 1251–1265. https://doi.org/10.1111/j.1365-2958.2004.04204.x

Kiefer, M., Neff, N., & Chamberlin, M. J. (1977). Transcriptional termination at the end of the early region of bacteriophages T3 and T7 is not affected by polarity suppressors. *Journal of Virology*, *22*(2), 548–552.

Kim, J.-S., Kim, S.-H., & Chung, Y.-B. (1997). Defects in Concatemer Processing of Bacteriophage T7 DNA Deleted in the M-Hairpin Region. *Virology*, *236*(1), 37–46. https://doi.org/10.1006/viro.1997.8715

Klusch, N., Murphy, B. J., Mills, D. J., Yildiz, Ö., & Kühlbrandt, W. (2017). Structural basis of proton translocation and force generation in mitochondrial ATP synthase. *ELife*, *6*, e33274. https://doi.org/10.7554/eLife.33274

Kronheim, S., Daniel-Ivad, M., Duan, Z., Hwang, S., Wong, A. I., Mantel, I., Nodwell, J. R., & Maxwell, K. L. (2018). A chemical defence against phage infection. *Nature*, *564*(7735), 283. https://doi.org/10.1038/s41586-018-0767-x

Krüger, D. H., & Schroeder, C. (1981). Bacteriophage T3 and bacteriophage T7 virus-host cell interactions. *Microbiological Reviews*, *45*(1), 9–51.

Kuhn, A., & Kellenberger, E. (1985). Productive phage infection in Escherichia coli with reduced internal levels of the major cations. *Journal of Bacteriology*, *163*(3), 906–912.

Kuo, M. M.-C., Saimi, Y., & Kung, C. (2003). Gain-of-function mutations indicate that Escherichia coli Kch forms a functional K+ conduit in vivo. *The EMBO Journal*, *22*(16), 4049–4058. https://doi.org/10.1093/emboj/cdg409

Labaw, L. W. (1951). THE ORIGIN OF PHOSPHORUS IN ESCHERICHIA COLI BACTERIOPHAGES. *Journal of Bacteriology*, *62*(2), 169–173.

Labaw, L. W. (1953). THE ORIGIN OF PHOSPHORUS IN THE T1, T5, T6, AND T7 BACTERIOPHAGES OF ESCHERICHIA COLI. *Journal of Bacteriology*, *66*(4), 429–436.

Lai, C.-J., & Nathans, D. (1974). Deletion mutants of simian virus 40 generated by enzymatic excision of DNA segments from the viral genome. *Journal of Molecular Biology*, *89*(1), 179–193. https://doi.org/10.1016/0022-2836(74)90169-7

Langman, L., & Paetkau, V. (1978). Purification and structures of recombining and replicating bacteriophage T7 DNA. *Journal of Virology*, *25*(2), 562–569.

Lazar, Jr, I., & Lazar, Sr, I. (n.d.). *Gel Analyzer 19.1*. www.gelanalyzer.com

Lee, D., & Sadowski, P. D. (1983). In vitro recombination of bacteriophage T7 DNA detected by a direct physical assay. *Journal of Virology*, *48*(3), 647–653.

Letellier, L., Plançon, L., Bonhivers, M., & Boulanger, P. (1999). Phage DNA transport across membranes. *Research in Microbiology*, *150*(8), 499–505. https://doi.org/10.1016/S0923-2508(99)00107-2

Liu, J., Hu, B., Morado, D. R., Jani, S., Manson, M. D., & Margolin, W. (2012). Molecular architecture of chemoreceptor arrays revealed by cryoelectron tomography of Escherichia coli minicells. *Proceedings of the National Academy of Sciences of the United States of America*, *109*(23), E1481–E1488. https://doi.org/10.1073/pnas.1200781109

Luria, S. E., & Delbrück, M. (1943). Mutations of Bacteria from Virus Sensitivity to Virus Resistance. *Genetics*, *28*(6), 491–511.

Makarova, K. S., Wolf, Y. I., Snir, S., & Koonin, E. V. (2011). Defense islands in bacterial and archaeal genomes and prediction of novel defense systems. *Journal of Bacteriology*, *193*(21), 6039–6056. https://doi.org/10.1128/JB.05535-11

Maloney, P. C., Kashket, E. R., & Wilson, T. H. (1974). A Protonmotive Force Drives ATP Synthesis in Bacteria. *Proceedings of the National Academy of Sciences*, *71*(10), 3896–3900. https://doi.org/10.1073/pnas.71.10.3896

Manson, M. D., Tedesco, P., Berg, H. C., Harold, F. M., & Van der Drift, C. (1977). A protonmotive force drives bacterial flagella. *Proceedings of the National Academy of Sciences of the United States of America*, *74*(7), 3060–3064.

Marinus, M. G., Poteete, A., & Arraj, J. A. (1984). *Correlation of DNA adenine methylase activity with spontaneous mutability in EscltericAiu coli K-12*. https://doi.org/10.1016/0378-1119(84)90095-7

Mark, D. F., & Richardson, C. C. (1976). Escherichia coli thioredoxin: A subunit of bacteriophage T7 DNA polymerase. *Proceedings of the National Academy of Sciences*, *73*(3), 780–784. https://doi.org/10.1073/pnas.73.3.780

Matson, S. W., & Richardson, C. C. (1985). Nucleotide-dependent binding of the gene 4 protein of bacteriophage T7 to single-stranded DNA. *The Journal of Biological Chemistry*, *260*(4), 2281–2287.

Maurer, L. M., Yohannes, E., Bondurant, S. S., Radmacher, M., & Slonczewski, J. L. (2005). PH Regulates Genes for Flagellar Motility, Catabolism, and Oxidative Stress in Escherichia coli K-12. *Journal of Bacteriology*, *187*(1), 304–319. https://doi.org/10.1128/JB.187.1.304-319.2005

Millette, R. L., Trotter, C. D., Herrlich, P., & Schweiger, M. (1970). In vitro Synthesis, Termination, and Release of Active Messenger RNA. *Cold Spring Harbor Symposia on Quantitative Biology*, *35*, 135–142. https://doi.org/10.1101/SQB.1970.035.01.020

Millman, A., Bernheim, A., Stokar-Avihail, A., Fedorenko, T., Voichek, M., Leavitt, A., Oppenheimer-Shaanan, Y., & Sorek, R. (2020). Bacterial Retrons Function In Anti-Phage Defense. *Cell*, *183*(6), 1551-1561.e12. https://doi.org/10.1016/j.cell.2020.09.065

Millman, A., Melamed, S., Leavitt, A., Doron, S., Bernheim, A., Hör, J., Garb, J., Bechon, N., Brandis, A., Lopatina, A., Ofir, G., Hochhauser, D., Stokar-Avihail, A., Tal, N., Sharir, S., Voichek, M., Erez, Z., Ferrer, J. L. M., Dar, D., … Sorek, R. (2022). An expanded arsenal of immune systems that protect bacteria from phages. *Cell Host & Microbe*, *30*(11), 1556-1569.e5. https://doi.org/10.1016/j.chom.2022.09.017

Modrich, P., & Richardson, C. C. (1975). Bacteriophage T7 deoxyribonucleic acid replication invitro. Bacteriophage T7 DNA polymerase: An an emzyme composed of phage- and host-specific subunits. *The Journal of Biological Chemistry*, *250*(14), 5515–5522.

Moffatt, B. A., & Studier, F. W. (1988). Entry of bacteriophage T7 DNA into the cell and escape from host restriction. *Journal of Bacteriology*, *170*(5), 2095–2105.

Mojica, F. J. M., Díez-Villaseñor, C., García-Martínez, J., & Soria, E. (2005). Intervening Sequences of Regularly Spaced Prokaryotic Repeats Derive from Foreign Genetic Elements. *Journal of Molecular Evolution*, *60*(2), 174–182. https://doi.org/10.1007/s00239-004-0046-3

Nechaev, S., & Severinov, K. (1999). Inhibition of Escherichia coli RNA polymerase by bacteriophage T7 gene 2 protein. *Journal of Molecular Biology*, *289*(4), 815–826. https://doi.org/10.1006/jmbi.1999.2782

Nguyen, V. S., Logger, L., Spinelli, S., Legrand, P., Huyen Pham, T. T., Nhung Trinh, T. T., Cherrak, Y., Zoued, A., Desmyter, A., Durand, E., Roussel, A., Kellenberger, C., Cascales, E., & Cambillau, C. (2017). Type VI secretion TssK baseplate protein exhibits structural similarity with phage receptor-binding proteins and evolved to bind the membrane complex. *Nature Microbiology*, *2*(9), Article 9. https://doi.org/10.1038/nmicrobiol.2017.103

Noji, H., Yasuda, R., Yoshida, M., & Kinosita, K. (1997). Direct observation of the rotation of F1-ATPase. *Nature*, *386*(6622), Article 6622. https://doi.org/10.1038/386299a0

North, R., & Molineux, I. J. (1980). A novel mutant of bacteriophage T7 that is defective in early phage DNA synthesis. *Molecular and General Genetics MGG*, *179*(3), 683–691. https://doi.org/10.1007/BF00271758

Paetkau, V., Langman, L., & Miller, R. C. (1975). The origin of nascent single-stranded fragments in replicating T7 DNA. *Journal of Molecular Biology*, *98*(4), 719–737. https://doi.org/10.1016/S0022-2836(75)80006-4

Pao, C.-C., & Speyer, J. F. (1973). Order of Injection of T7 Bacteriophage DNA. *Journal of Virology*, *11*(6), 1024–1026.

Parikka, K. J., Le Romancer, M., Wauters, N., & Jacquet, S. (2017). Deciphering the virus-to-prokaryote ratio (VPR): Insights into virus–host relationships in a variety of ecosystems. *Biological Reviews*, *92*(2), 1081–1100. https://doi.org/10.1111/brv.12271

Paul, K., Erhardt, M., Hirano, T., Blair, D. F., & Hughes, K. T. (2008). Energy source of flagellar type III secretion. *Nature*, *451*(7177), Article 7177. https://doi.org/10.1038/nature06497

Pezo, V., Jaziri, F., Bourguignon, P.-Y., Louis, D., Jacobs-Sera, D., Rozenski, J., Pochet, S., Herdewijn, P., Hatfull, G. F., Kaminski, P.-A., & Marliere, P. (2021). Noncanonical DNA polymerization by aminoadenine-based siphoviruses. *Science*, *372*(6541), 520–524. https://doi.org/10.1126/science.abe6542

Ptashne, M. (1967). ISOLATION OF THE λ PHAGE REPRESSOR*. *Proceedings of the National Academy of Sciences of the United States of America*, *57*(2), 306–313.

R Core Team. (2021). *R: A Language and Environment for Statistical Computing* (4.1.2). R Foundation for Statistical Computing. https://www.R-project.org/

Rabkin, S. D., & Richardson, C. C. (1988). Initiation of DNA replication at cloned origins of bacteriophage T7. *Journal of Molecular Biology*, *204*(4), 903–916. https://doi.org/10.1016/0022-2836(88)90050-2

Romano, L. J., Tamanoi, F., & Richardson, C. C. (1981). Initiation of DNA replication at the primary origin of bacteriophage T7 by purified proteins: Requirement for T7 RNA polymerase. *Proceedings of the National Academy of Sciences of the United States of America*, *78*(7), 4107–4111. https://doi.org/10.1073/pnas.78.7.4107

Roux, S., Krupovic, M., Daly, R. A., Borges, A. L., Nayfach, S., Schulz, F., Sharrar, A., Matheus Carnevali, P. B., Cheng, J.-F., Ivanova, N. N., Bondy-Denomy, J., Wrighton, K. C., Woyke, T., Visel, A., Kyrpides, N. C., & Eloe-Fadrosh, E. A. (2019). Cryptic inoviruses revealed as pervasive in bacteria and archaea across Earth's biomes. *Nature Microbiology*, *4*(11), 1895–1906. https://doi.org/10.1038/s41564-019-0510-x

RStudio Team. (2022). *RStudio: Integrated Development Environment for R* (2022.7.2.576). RStudio, PBC. http://www.rstudio.com/

Ryals, J., Little, R., & Bremer, H. (1982). Temperature dependence of RNA synthesis parameters in Escherichia coli. *Journal of Bacteriology*, *151*(2), 879–887.

Sadowski, P. D., & Kerr, C. (1970). Degradation of Escherichia coli B Deoxyribonucleic Acid After Infection with Deoxyribonucleic Acid-Defective Amber Mutants of Bacteriophage T7. *Journal of Virology*, *6*(2), 149–155. https://doi.org/10.1128/jvi.6.2.149-155.1970

Saito, H., Tabor, S., Tamanoi, F., & Richardson, C. C. (1980). Nucleotide sequence of the primary origin of bacteriophage T7 DNA replication: Relationship to adjacent genes and regulatory elements. *Proceedings of the National Academy of Sciences of the United States of America*, *77*(7), 3917–3921.

Salmond, C. V., Kroll, R. G., & Booth, I. R. (1984). The effect of food preservatives on pH homeostasis in Escherichia coli. *Journal of General Microbiology*, *130*(11), 2845–2850. https://doi.org/10.1099/00221287-130-11-2845

Schlesinger, M. (1932a). Die Bestimmung von Teilchengröße und spezifischem Gewicht des Bakteriophagen durch Zentrifugierversuche. *Zeitschrift für Hygiene und Infektionskrankheiten*, *114*(1), 161–176. https://doi.org/10.1007/BF02176516

Schlesinger, M. (1932b). Über die Bindung des Bakteriophagen an homologe Bakterien. *Zeitschrift für Hygiene und Infektionskrankheiten*, *114*(1), 136–148. https://doi.org/10.1007/BF02176514

Schlesinger, M. (1933a). Beobachtung und Zählung von Bakteriophagenteilchen im Dunkelfeld. —Die Form der Teilchen. *Zeitschrift für Hygiene und Infektionskrankheiten*, *115*(4), 774–780. https://doi.org/10.1007/BF02176805

Schlesinger, M. (1933b). Reindarstellung eines Bakteriophagen in mit freiem Auge sichtbaren Mengen. *Biochem. Z*, *264*, 6.

Schlesinger, M. (1934). Zur Frage der chemischen Zusammensetzung des Bakteriophagen. *Biochem. Z*, *273*, 306.

Schlesinger, M. (1936). The Feulgen Reaction of the Bacteriophage Substance. *Nature*, *138*(3490), Article 3490. https://doi.org/10.1038/138508c0

Schneider, C. A., Rasband, W. S., & Eliceiri, K. W. (2012). NIH Image to ImageJ: 25 years of image analysis. *Nature Methods*, *9*(7), Article 7. https://doi.org/10.1038/nmeth.2089

Schrödinger, E., Schrödinger, E., & Schrödinger, E. (1992). *What is life? The physical aspect of the living cell ; with, Mind and matter ; & Autobiographical sketches*. Cambridge University Press.

Schultz, S. G., & Solomon, A. K. (1961). Cation transport in Escherichia coli. I. Intracellular Na and K concentrations and net cation movement. *The Journal of General Physiology*, *45*(2), 355–369. https://doi.org/10.1085/jgp.45.2.355

Serwer, P. (1976). Internal proteins of bacteriophage T7. *Journal of Molecular Biology*, *107*(3), 271–291. https://doi.org/10.1016/S0022-2836(76)80005-8

Serwer, P., Wright, E. T., Hakala, K. W., & Weintraub, S. T. (2008). Evidence for bacteriophage T7 tail extension during DNA injection. *BMC Research Notes*, *1*, 36. https://doi.org/10.1186/1756-0500-1-36

Siddiqi, M. S. H., Kozloff, L. M., Putnam, F. W., & Evans, E. A. (1952). Biochemical studies of virus reproduction. IX. Nature of the host cell contributions. *The Journal of Biological Chemistry*, *199*(1), 165–176.

Simon, M. N., & Studier, F. W. (1973). Physical mapping of the early region of bacteriophage T7 DNA. *Journal of Molecular Biology*, *79*(2), 249–265. https://doi.org/10.1016/0022-2836(73)90004-1

Sleiman, D., Garcia, P. S., Lagune, M., Loc'h, J., Haouz, A., Taib, N., Röthlisberger, P., Gribaldo, S., Marlière, P., & Kaminski, P. A. (2021). A third purine biosynthetic pathway encoded by aminoadenine-based viral DNA genomes. *Science*, *372*(6541), 516–520. https://doi.org/10.1126/science.abe6494

Slonczewski, J. L., Fujisawa, M., Dopson, M., & Krulwich, T. A. (2009). Cytoplasmic pH Measurement and Homeostasis in Bacteria and Archaea. In R. K. Poole (Ed.), *Advances in Microbial Physiology* (Vol. 55, pp. 1–317). Academic Press. https://doi.org/10.1016/S0065-2911(09)05501-5

Slonczewski, J. L., Rosen, B. P., Alger, J. R., & Macnab, R. M. (1981). pH homeostasis in Escherichia coli: Measurement by 31P nuclear magnetic resonance of methylphosphonate and phosphate. *Proceedings of the National Academy of Sciences of the United States of America*, *78*(10), 6271–6275. https://doi.org/10.1073/pnas.78.10.6271

Smith, H. O., & Wilcox, K. W. (1970). A restriction enzyme from Hemophilus influenzae. I. Purification and general properties. *Journal of Molecular Biology*, *51*(2), 379–391. https://doi.org/10.1016/0022-2836(70)90149-x

Stent, G. (1963). *Molecular biology of bacterial viruses*. Freeman. https://www.ncbi.nlm.nih.gov/nlmcatalog/308475

Steven, A. C., Trus, B. L., Maizel, J. V., Unser, M., Parry, D. A., Wall, J. S., Hainfeld, J. F., & Studier, F. W. (1988). Molecular substructure of a viral receptor-recognition protein. The gp17 tail-fiber of bacteriophage T7. *Journal of Molecular Biology*, *200*(2), 351–365. https://doi.org/10.1016/0022-2836(88)90246-x

Steven, A., & Trus, B. (1986). The structure of bacteriophage T7. In J. Harris & R. Horne (Eds.), *Electron Microscopy of Proteins: Viral Structure: Vol. Vol. 5* (pp. 1–33). Academic Press.

Stroud, R. M., Serwer, P., & Ross, M. J. (1981). Assembly of bacteriophage T7. Dimensions of the bacteriophage and its capsids. *Biophysical Journal*, *36*(3), 743–757.

Struthers-Schlinke, J. S., Robins, W. P., Kemp, P., & Molineux, I. J. (2000a). The internal head protein Gp16 controls DNA ejection from the bacteriophage T7 virion. *Journal of Molecular Biology*, *301*(1), 35–45. https://doi.org/10.1006/jmbi.2000.3940

Struthers-Schlinke, J. S., Robins, W. P., Kemp, P., & Molineux, I. J. (2000b). The internal head protein Gp16 controls DNA ejection from the bacteriophage T7 virion11Edited by M. Gottesman. *Journal of Molecular Biology*, *301*(1), 35–45. https://doi.org/10.1006/jmbi.2000.3940

Studier, F. W. (1969). The genetics and physiology of bacteriophage T7. *Virology*, *39*(3), 562–574. https://doi.org/10.1016/0042-6822(69)90104-4

Studier, F. W. (1972). Bacteriophage T7. *Science (New York, N.Y.)*, *176*(4033), 367–376. https://doi.org/10.1126/science.176.4033.367

Studier, F. W., & Moffatt, B. A. (1986). Use of bacteriophage T7 RNA polymerase to direct selective high-level expression of cloned genes. *Journal of Molecular Biology*, *189*(1), 113–130. https://doi.org/10.1016/0022-2836(86)90385-2

Susman, M. (1995). The Cold Spring Harbor Phage Course (1945-1970): A 50th Anniversary Remembrance. *Genetics*, *139*(3), 1101–1106.

Suzuki, T., Ueno, H., Mitome, N., Suzuki, J., & Yoshida, M. (2002). F0 of ATP Synthase Is a Rotary Proton Channel: OBLIGATORY COUPLING OF PROTON TRANSLOCATION WITH ROTATION OF c-SUBUNIT RING∗. *Journal of Biological Chemistry*, *277*(15), 13281–13285. https://doi.org/10.1074/jbc.M111210200

Tabor, S., & Richardson, C. C. (1981). Template recognition sequence for RNA primer synthesis by gene 4 protein of bacteriophage T7. *Proceedings of the National Academy of Sciences of the United States of America*, *78*(1), 205–209. https://doi.org/10.1073/pnas.78.1.205

Tabor, S., & Richardson, C. C. (1985). A bacteriophage T7 RNA polymerase/promoter system for controlled exclusive expression of specific genes. *Proceedings of the National Academy of Sciences of the United States of America*, *82*(4), 1074–1078. https://doi.org/10.1073/pnas.82.4.1074

Tabor, S., & Richardson, C. C. (1987). DNA sequence analysis with a modified bacteriophage T7 DNA polymerase. *Proceedings of the National Academy of Sciences*, *84*(14), 4767–4771. https://doi.org/10.1073/pnas.84.14.4767

Takekawa, N., Terahara, N., Kato, T., Gohara, M., Mayanagi, K., Hijikata, A., Onoue, Y., Kojima, S., Shirai, T., Namba, K., & Homma, M. (2016). The tetrameric MotA complex as the core of the flagellar motor stator from hyperthermophilic bacterium. *Scientific Reports*, *6*, 31526. https://doi.org/10.1038/srep31526

Tal, N., Morehouse, B. R., Millman, A., Stokar-Avihail, A., Avraham, C., Fedorenko, T., Yirmiya, E., Herbst, E., Brandis, A., Mehlman, T., Oppenheimer-Shaanan, Y., Keszei, A. F. A., Shao, S., Amitai, G., Kranzusch, P. J., & Sorek, R. (2021). Cyclic CMP and cyclic UMP mediate bacterial immunity against phages. *Cell*, *184*(23), 5728-5739.e16. https://doi.org/10.1016/j.cell.2021.09.031

TBE buffer. (2006). *Cold Spring Harbor Protocols*, *2006*(1), pdb.rec8458. https://doi.org/10.1101/pdb.rec8458

Thomas, J. D., Daniel, R. A., Errington, J., & Robinson, C. (2001). Export of active green fluorescent protein to the periplasm by the twin-arginine translocase (Tat) pathway in Escherichia coli. *Molecular Microbiology*, *39*(1), 47–53. https://doi.org/10.1046/j.1365-2958.2001.02253.x

Twort, F. W. (1915). AN INVESTIGATION ON THE NATURE OF ULTRA-MICROSCOPIC VIRUSES. *The Lancet*, *186*(4814), 1241–1243. https://doi.org/10.1016/S0140-6736(01)20383-3

*Type VI secretion system translocates a phage tail spike-like protein into target cells where it cross-links actin | PNAS*. (n.d.). Retrieved June 7, 2023, from https://www-pnas-org.ezproxy.lib.utexas.edu/doi/full/10.1073/pnas.0706532104

Visconti, N., & Delbrück, M. (1953). The Mechanism of Genetic Recombination in Phage. *Genetics*, *38*(1), 5–33.

Vogel, U., & Jensen, K. F. (1994). The RNA chain elongation rate in Escherichia coli depends on the growth rate. *Journal of Bacteriology*, *176*(10), 2807–2813. https://doi.org/10.1128/jb.176.10.2807-2813.1994

Vogel, U., & Jensen, K. F. (1997). NusA Is Required for Ribosomal Antitermination and for Modulation of the Transcription Elongation Rate of both Antiterminated RNA and mRNA*. *Journal of Biological Chemistry*, *272*(19), 12265–12271. https://doi.org/10.1074/jbc.272.19.12265

Watson, J. D. (1972). Origin of Concatemeric T7DNA. *Nature New Biology*, *239*(94), Article 94. https://doi.org/10.1038/newbio239197a0

White, J. H., & Richardson, C. C. (1987). Processing of concatemers of bacteriophage T7 DNA in vitro. *Journal of Biological Chemistry*, *262*(18), 8851–8860. https://doi.org/10.1016/S0021-9258(18)47493-5

Wiedenmann, A., Dimroth, P., & von Ballmoos, C. (2008). Δψ and ΔpH are equivalent driving forces for proton transport through isolated F0 complexes of ATP synthases. *Biochimica et Biophysica Acta (BBA) - Bioenergetics*, *1777*(10), 1301–1310. https://doi.org/10.1016/j.bbabio.2008.06.008

Wilks, J. C., & Slonczewski, J. L. (2007). pH of the Cytoplasm and Periplasm of Escherichia coli: Rapid Measurement by Green Fluorescent Protein Fluorimetry. *Journal of Bacteriology*, *189*(15), 5601–5607. https://doi.org/10.1128/JB.00615-07

Wolfson, J., Dressler, D., & Magazin, M. (1972). Bacteriophage T7 DNA replication: A linear replicating intermediate (gradient centrifugation-electron microscopy-E. coli-DNA partial denaturation). *Proceedings of the National Academy of Sciences of the United States of America*, *69*(2), 499–504. https://doi.org/10.1073/pnas.69.2.499

Zavriev, S. k., & Shemyakin, M. f. (1981). Influence of the deletions of A2–A3 promoters or a terminator of early genes upon the rate of T7 DNA entrance into Escherichia coli cell. *FEBS Letters*, *131*(1), 99–102. https://doi.org/10.1016/0014-5793(81)80896-4

Zavriev, S. K., & Shemyakin, M. F. (1982). RNA polymerase-dependent mechanism for the stepwise T7 phage DNA transport from the virion into E. coli. *Nucleic Acids Research*, *10*(5), 1635–1652.

Zavriev, S. K., & Vorob'ev, S. M. (n.d.). *Evidence for the coupling of T7 DNA injection with its transcription during infection*. https://doi.org/10.1016/0014-5793(84)80008-3

Zhang, X., & Studier, F. W. (2004). Multiple Roles of T7 RNA Polymerase and T7 Lysozyme During Bacteriophage T7 Infection. *Journal of Molecular Biology*, *340*(4), 707–730. https://doi.org/10.1016/j.jmb.2004.05.006

Zhou, Y., Duncan, T. M., & Cross, R. L. (1997). Subunit rotation in Escherichia coli FoF1–ATP synthase during oxidative phosphorylation. *Proceedings of the National Academy of Sciences*, *94*(20), 10583–10587. https://doi.org/10.1073/pnas.94.20.10583

Zhou, Y., Xu, X., Wei, Y., Cheng, Y., Guo, Y., Khudyakov, I., Liu, F., He, P., Song, Z., Li, Z., Gao, Y., Ang, E. L., Zhao, H., Zhang, Y., & Zhao, S. (2021). A widespread

pathway for substitution of adenine by diaminopurine in phage genomes. *Science*, *372*(6541), 512–516. https://doi.org/10.1126/science.abe4882

Zillig, W., Fujiki, H., Blum, W., Janeković, D., Schweiger, M., Rahmsdorf, H., Ponta, H., & Hirsch-Kauffmann, M. (1975). In vivo and in vitro phosphorylation of DNA-dependent RNA polymerase of Escherichia coli by bacteriophage-T7-induced protein kinase. *Proceedings of the National Academy of Sciences of the United States of America*, *72*(7), 2506–2510. https://doi.org/10.1073/pnas.72.7.2506